Botrytis cinerea BcPTP1 is a late infection phase, cysteine rich protein cytotoxic effector

Wenjun Zhu[1]*, Mengxue Yu[1], Ran Xu[1], Kai Bi[1], Chao Xiong[1], Zhiguo Liu[1], Amir Sharon[2], Daohong Jiang[3], Mingde Wu[3], Qiongnan Gu[4], Ling Gong[5], Weidong Chen[6], Wei Wei[6]*

1. School of Life Science and Technology, Wuhan Polytechnic University, Wuhan 430023, Hubei Province, China.

2. School of Plant Sciences and Food Security, Faculty of Life Sciences, Tel Aviv University, Tel Aviv 69978, Israel.

3. State Key Laboratory of Agricultural Microbiology, Huazhong Agricultural University, Wuhan 430070, Hubei Province, China.

4. Institute of Plant Protection and Soil Fertilizer, Hubei Academy of Agricultural Sciences/Key Laboratory of Integrated Pest Management on Crops in Central China, Ministry of Agriculture and Rural Affairs/Hubei Key Laboratory of Crop Diseases, Insect Pests and Weeds control, Wuhan 430064, Hubei Province, China.

5. Pharmacy Faculty, Hubei University of Chinese Medicine, Wuhan 430065, Hubei Province, China.

6. Department of Plant Pathology, Washington State University, United States Department of Agriculture-Agricultural Research Service, Washington State University, Pullman 99164, USA.

*Corresponding authors.

E-mail addresses:

Wenjun Zhu: zhuwenjun2017@whpu.edu.cn

Wei Wei: wei.wei2@wsu.edu

Abstract

Botrytis cinerea is a broad-host-range necrotrophic phytopathogen responsible for serious crops diseases. To facilitate infection, *B. cinerea* secretes a large number of effectors that induce plant cell death. In screening secretome data of *B. cinerea* during infection stage, we identified a phytotoxic protein (BcPTP1) that can also induce immune resistance in plants. BcPTP1 is a small (90 aa), cysteine rich protein without any known domains. Transiently expression of BcPTP1 in leaves caused chlorosis that intensifies with time and eventually lead to cell death. Point mutations in eight of the 10 cysteine residues of BcPTP1 abolished the toxic effect, however residual toxic activity remained after heating the peptide, suggesting contribution of unknown epitopes to protein phytotoxic effect. The transcript level of the *bcptp1* gene was low during the first 36 h after inoculation and increased sharply upon transition to the late infection stage, suggesting a role of BcPTP1 in lesion spreading. While statistically insignificant, deletion of the *bcptp1* gene led to slightly smaller lesions on bean leaves. Further analyses indicated that BcPTP1 is internalized into plant cells after secreting into the apoplast and its phytotoxic effect is negatively regulated by the receptor-like kinases BAK1 and SOBIR1. Collectively, our findings show that BcPTP1 is a virulence factor that toxifies the host cells and facilitates lesion spreading during the late infection stage.

Keywords: *Botrytis cinerea*, effector, cell death, phytotoxic protein, immune resistance, receptor-like kinases

Introduction

During the evolutionary arms race with phytopathogens, plants have developed a sophisticated defense system (Jones and Dangl, 2006). The first defense layer is pathogen-associated molecular patterns (PAMPs)-triggered immunity (PTI), in which host receptors recognize molecules or domains that are conserved in certain groups of pathogens and induce an effective resistance response (Albert *et al.*, 2020). In fungi and oomycetes, the best studied PAMPs include glucans (Fliegmann *et al.*, 2004), xylanase EIX (Rotblat *et al.*, 2002), chitin (Shinya *et al.*, 2015), endopolygalacturonases (Zhang *et al.*, 2014b), Pep13 (Brunner *et al.*, 2002), Cerato-platanin proteins (Yang *et al.*, 2018) and INF1 (Kanneganti *et al.*, 2006). In addition, several PAMPs that induce plant necrosis or PTI across different classes of microbes have also been well characterized, such as glycoside hydrolase 12 proteins (GH12) in the fungal pathogen *Verticillium dahliae* and *Botrytis cinerea* (Gui *et al.*, 2017; Zhu *et al.*, 2017) and the oomycete pathogen *Phytophthora sojae* (Ma *et al.*, 2015; Ma *et al.*, 2017; Wang *et al.*, 2018), Ave1 protein in multiple plant pathogenic fungi and bacteria (Thomma *et al.*, 2011; de Jonge *et al.*, 2012), and the classical necrosis and ethylene-inducing peptide 1-like proteins (NLPs) in multiple prokaryotic and eukaryotic microbial pathogens (Oome *et al.*, 2014; Albert *et al.*, 2015).

To overcome the basal plant immunity and infect hosts effectively, biotrophic and hemibiotrophic pathogens secrete diverse effectors to the interface area between fungal hyphae and host or into plant cells (Stergiopoulos and de Wit, 2009; Lo Presti *et al.*, 2015; Kim *et al.*, 2016). To cope with pathogen effectors, plants have co-evolved a second line of defense, also called effector-triggered immunity (ETI), which is mediated by resistance (R) proteins and is often associated with the local plant cells hypersensitive response (HR) at the infection site (Cui *et al.*, 2015). HR is efficient in restricting biotrophic and hemibiotrophic pathogens (Jones and Dangl, 2006; van Ooijen *et al.*, 2007; Cui *et al.*, 2015), but is ineffective against necrotrophic pathogens, which can turn it against the host to facilitate infection (Lorang *et al.*, 2012; Gao *et al.*, 2015).

Compared to the large number and well characterized effectors in biotrophic and hemibiotrophic fungal pathogens, relatively fewer effectors have been studied in necrotrophic fungal pathogens, especially the broad-host-range necrotrophic fungal pathogens. *Botrytis cinerea* is a typical broad-host-range necrotrophic fungal phytopathogen, causing gray mold and rot diseases in hundreds of plant species including many agriculturally important crops, and leading to enormous economic losses each year (Dean *et al.*, 2012; Veloso and van Kan, 2018). It was shown that the infection process of *B. cinerea* on host plant includes three typical stages: an early stage characterized by local necrosis lesions formation, an intermediate stage during

which a variety of sophisticated interactions between plant-pathogen occur and determine the outcome of *B. cinerea* infections, and the late stage of fast-spreading lesions (Eizner *et al.*, 2017). Since *B. cinerea* infects and colonizes by killing plant cells, it secretes diverse effector proteins to manipulate the host defenses and/or to induce death for facilitating infection on host plants (Heard *et al.*, 2015; Frías *et al.*, 2016; Zhu *et al.*, 2017; Denton-Giles *et al.*, 2020; Frías *et al.*, 2011; Shao *et al.*, 2021). These secreted effector proteins play important roles during *Botrytis*-plant interactions. However, compared with biotrophic and hemibiotrophic pathogens effectors, the underlying biochemical activities and molecular mechanisms of the necrotrophic secreted proteins remain incompletely understood.

Aiming to characterize potential effectors of *B. cinerea*, we identified a secreted protein with a phytotoxic activity that was named BcPTP1 (phytotoxic protein). Similar to most other cell death inducing proteins (CDIPs, Li *et al.*, 2020; Shao *et al.*, 2021), BcPTP1 functions in apoplastic space of plant cell and induces a plant defense response. However, unlike the vast majority of CDIPs, BcPTP1 leads to development of gradual chlorosis rather than instant cell death and the *bcptp1* gene is expressed late during infection and affects lesion development, namely it is a late-stage virulence factor.

Results

BcPTP1 is a secreted protein with phytotoxic activity

The effect of putative effector proteins was tested by *Agrobacterium tumefaciens*-mediated transient expression (agroinfiltration) of the candidate proteins fused with GFP tag at the C-terminus in *N. benthamiana* leaves. We found that the protein BcPTP1 (BCIN_05g03680)-GFP containing a potential N-terminal signal peptide caused chlorosis in *N. benthamiana* leaves that developed within 10 days after agroinfiltration, eventually leading to cell death within 15 days after agroinfiltration (Fig. 1). Transient expression of BcPTP1$^{\Delta SP}$-GFP without the secretion signal peptide did not trigger leaf chlorosis, indicating that BcPTP1 may function in the leaf apoplastic space. This phenotype differs from the induction of necrotic cell death that is common to previously characterized apoplastic CDIPs (Li *et al.*, 2020; Shao *et al.*, 2021), and suggests that BcPTP1 has a phytotoxic activity rather than a necrotic cell death inducing activity.

Two methods were used to verify whether BcPTP1 is a secreted protein. First, the BcPTP1 signal peptide (initial N terminus 19 amino acids) was used to replace the N-terminal signal peptide of BcXYG1, the strong death-inducing secreted protein of *B. cinerea* which functions in the apoplastic space (Zhu *et al.*, 2017), to produce SP$^{(BcPTP1)}$-BcXYG1$^{\Delta SP}$-HA. The BcXYG1-HA with its native signal peptide was used

as a positive control, and the BcXYG1$^{\Delta SP}$-HA, GFP-HA, SP$^{(BcPTP1)}$-GFP-HA and empty vector were used as negative controls. Within five days after agroinfiltration, both of BcXYG1-HA and SP$^{(BcPTP1)}$-BcXYG1$^{\Delta SP}$-HA fusion proteins, which are secreted from the plant cells to the extracellular space, triggered typical plant cell death, whereas BcXYG1$^{\Delta SP}$-HA, which lacks the signal peptide and therefore remains inside the plant cell, failed to induce cell death (Fig. 2A). In the second method, we fused the signal peptide of BcPTP1 to GFP to form SP$^{(BcPTP1)}$-GFP. Likewise, we fused the signal peptide of BcXYG1 to GFP to form SP$^{(BcXYG1)}$-GFP for comparison. The constructs were used to transform the wild type *B. cinerea* strain to generate overexpression strains of these fusion proteins. All the indicated proteins were successfully expressed in the hyphae of each strain as shown in western blot analysis (Fig. 2C). Then, all examined strains were cultured in potato dextrose broth (PDB) for 3 days, the culture filtrates were collected, purified and presence of the fused proteins was checked by western blot analysis. The results confirmed the accumulation of GFP protein in the culture medium of SP$^{(BcPTP1)}$-GFP and SP$^{(BcXYG1)}$-GFP overexpression strains, but not the GFP overexpression or wild type (WT) strain (Fig. 2D). Collectively, these analyses confirmed the secretion function of the BcPTP1 signal peptide.

BcPTP1 is internalized into plant cell

The above results showed that BcPTP1 is a secreted protein and its phytotoxic activity depends on localization in the leaf apoplastic space (Fig. 1; Fig. 2). Thus, we postulated that BcPTP1 remains the in apoplastic space after secretion by the fungus. To verify this hypothesis, we analyzed the subcellular localization of BcPTP1-GFP fusion protein following agroinfiltration. Unexpectedly, we found that the BcPTP1-GFP fusion protein was mainly localized at the cytoplasmic vesicles and in the periphery of plant cell plasma membrane, whereas the BcPTP1$^{\Delta SP}$-GFP and GFP were mainly distributed in the nuclei and cytoplasm, and the SP^{BcPTP1}-GFP was concentrated in the apoplastic space (Fig. 3). The unexpected localization of BcPTP1 indicates that besides phytotoxic activity in apoplast, BcPTP1 can be also internalized into plant cells for other unknown functions after the initial secretion to apoplastic space.

BcPTP1 is toxic to dicot but not monocot plants

To determine whether BcPTP1 affects plants other than *N. benthamiana* and to avoid the *A. tumefaciens* incompatibility issues on plants, we produced and purified the BcPTP1 protein from *Escherichia coli* (Supplementary Fig. S1). Infiltration assay with different concentrations of the purified protein demonstrated that 25 µg/ml of BcPTP1 recombinant protein was sufficient to trigger leaf chlorosis in *N.*

benthamiana (Fig. 4A). Cell death developed following treatment of the leaves with higher protein titers (50-100 μg/ml). In addition, BcPTP1 also induced cell death in tomato and *A. thaliana* leaves, but not in the monocot maize even at high protein concentrations (Fig. 4B). These results indicated that BcPTP1 is toxic to multiple dicot plants, but not to monocot cereal.

Cysteine residues in BcPTP1 are important for protein toxicity

bcptp1 is a single-copy gene in *B. cinerea*, encoding 90 amino acids with 10 cysteine residues, out of which eight residues are highly conserved (Supplementary Fig. S2). Bioinformatics analysis demonstrated that the first 20 N-terminal amino acids encode a signal peptide. No other known protein domains or possible functions were predicted using ***SMART MODE*** analysis (http://smart.embl-heidelberg.de/smart/change_mode.pl), and also no nuclear localization signal or chloroplast transit peptide were found in protein sequence. BLAST searches against the **NCBI** database with the BcPTP1 sequence as query showed that homologs of BcPTP1 with high similarity are only present in a small number of fungal genera, most of which are plant pathogens, including *Botryotinia*, *Sclerotinia*, *Alternaria*, *Bipolaris*, *Fusarium*, *Colletotrichum*, *Botrytis*, and saprotrophic *Aspergillus* species. Significantly, no homologs were found in any of the biotrophic plant pathogens or in human pathogenic fungi. Multiple sequence alignment and phylogenetic analysis of BcPTP1 and its homologues showed significant sequence similarity (Supplementary Fig. S2A and S2B). 3D structure prediction of BcPTP1 using *I-TASSER* showed that BcPTP1 contains two α-helices on each side of the protein structure and two internal β-strands (Supplementary Fig. S2C).

Many effectors are small secreted cysteine-rich proteins (SSCP). The cysteine residues contribute to the formation of disulfide bonds (Sevier and Kaiser, 2002; Marianayagam *et al.*, 2004), which are essential for the structure and function of these proteins (Stergiopoulos and de Wit, 2009). To examine whether phytotoxicity of BcPTP1 depends on its cysteine residues, we replaced each of the 10 cysteine residues with alanine individually using site-directed mutagenesis. *A. tumefaciens* infiltration assay of *N. benthamiana* leaves demonstrated that mutations of C26A or C34A individually could induce more severe phenotype than the native BcPTP1 protein. The activity of the C67A mutant decreased compared to the native protein, whereas mutations in any of the seven remaining cysteine residues completely abolished phytotoxicity (Fig. 5). Additionally, boiling the BcPTP1 protein at 100□ for 30 min reduced, but did not completely abolished phytotoxicity (Fig. 6). These results suggest that certain epitopes, which are affected by specific cysteine residues, mediate the phytotoxic activity of the BcPTP1 protein.

bcptp1 is highly expressed at late infection stage but is not essential for pathogenicity

To analyze the biological roles of BcPTP1 during *B. cinerea* infection, we measured the expression levels of the *bcptp1* gene during infection. The transcript levels of *bcptp1* were low at early infection stage and then increased sharply about 48 hpi with a peak at 60 hpi, about 35-fold higher than at 0 hpi (Fig. 7). When *B. cinerea* was cultured on solid Gamborg's B5 medium, the transcript level of *bcptp1* was increased about 12-fold at 36 hpi compared to earlier time points, and then remained stable throughout the culture period (Fig. 7).

To further investigate possible role of BcPTP1 in *B. cinerea* pathogenicity, we generated *bcptp1* gene deletion and overexpression strains (Supplementary Fig. S3). All the deletion and overexpression strains had normal colony morphology, conidia production and growth rate on potato dextrose agar (PDA) (Supplementary Fig. S4). In addition, we did not observe obvious changes in sensitivity of the transgenic strains to various types of stresses, including 1 M NaCl, 1 M sorbitol, 0.02% SDS, 20 mM H_2O_2, 0.3 mg/ml Calcofluor White and 0.5 mg/ml Congo Red (Supplementary Fig. S5).

Pathogenicity study showed that the *bcptp1* deletion strains caused slightly smaller disease lesion on bean leaves than the wild type strain, although the differences were statistically insignificant (Supplementary Fig. S6). Likewise, the *bcptp1* over expression strains did not show obvious difference in lesion size (Supplementary Fig. S6). The results indicated that deletion or overexpression of *bcptp1* does not significantly affect the final outcome of *B. cinerea* infection.

BcPTP1 triggers immune response and induces resistance against *B. cinerea* in *N. benthamiana*

High proportion of the analyzed CDIPs are recognized by the plant immune system and activate a defense response. To analyze whether BcPTP1 can induce plant resistance to *B. cinerea*, *N. benthamiana* leaves were infiltrated with 10 μg/ml of purified BcPTP1 or GFP proteins, 48 h later, the infiltrated leaves were inoculated with *B. cinerea* mycelia plugs, the plants were incubated for an additional 48 h in a moist chamber and then symptoms were recorded. The results showed that the infection on tobacco leaves pre-treated with BcPTP1 protein was significantly reduced compared to leaves pre-treated with GFP protein (Fig. 8A), indicating that along with phytotoxicity, BcPTP1 can also trigger plant resistance.

To verify whether the enhanced resistance of tobacco caused by BcPTP1 is associated with the expression changes of defense-related genes, we analyzed the transcript alteration of salicylic acid (SA) signal pathway genes *NbPR1a* and *NbPR2*,

Jasmonic acid (JA) signal pathway genes *NbPR4* and *NbLOX*, ethylene signal pathway gene *NbERF1*, HR-related genes *HIN1*, and PTI-related genes *NbWRKY7* and *NbPTI5* using RT-qPCR, as previously described (Nie *et al.*, 2019). In all cases we observed a drastic increase in gene expression after infiltration of the leaves with 10 μg/ml BcPTP1 (Fig. 8B).

BAK1 and SOBIR1 negatively regulate the death-inducing activity of BcPTP1 in *N. benthamiana*

Since BcPTP1 is targeted to the apoplast space of *N. benthamiana* tissue, it is possible that similar to other CDIPs, BcPTP1 interacts with plant membrane receptor-like proteins (RLPs) to transmit the immunity signals via the RLP-SOBIR1-BAK1 complex (Liebrand *et al.*, 2013; Zhang *et al.*, 2014b; Albert *et al.*, 2015; Ma *et al.*, 2015; Postma *et al.*, 2016; Gui *et al.*, 2017; Zhu *et al.*, 2017). To test this possibility, we generated *NbBAK1*- and *NbSOBIR1*-silenced *N. benthamiana* plants using virus-induced gene silencing (VIGS). The gene-silenced plants were agroinfiltrated with BcPTP1 expression construct. Unexpectedly, BcPTP1 induced a much more severe phytotoxicity in the *BAK1*- or *SOBIR1*-silenced plants than in wild type tobacco plants (Fig. 9). The result indicated that the death-inducing signal of BcPTP1 is mediated through an unknown signal transduction pathway, and is negatively regulated by BAK1 and SOBIR1.

Discussion

The search for *B. cinerea* cell death-inducing effectors has yielded an increasing number of candidates DCIPs, most of which are associated with production of local necrosis during the early infection stage (Li *et al.*, 2020; Shao *et al.*, 2021). In search of factors that facilitate disease progression in late infection stage (lesion spreading), we identified BcPTP1, a SSCP with phytotoxic activity, which is expressed at the late infection stage. As such, BcPTP1 fulfills the definition of a late-stage necrotrophic effector.

The late *in planta* induction of *bcptp1* (Fig. 7) supports a potential role of BcPTP1 in the pathogenicity of *B. cinerea* at the late infection stage, probably as a factor that facilitates lesion expansion. Since the BcPTP1 is recognized by the plant immune system (Fig. 8), the late expression of the *bcptp1* gene might also prevent early perception and induction of a plant defense response. Despite the phytoxicity and induction *in planta*, deletion of *bcptp1* gene had only minor effect on fungal virulence (Supplementary Fig. S6). Such minor, or even lack of a visible change in virulence is common to many fungal effectors, and probably reflects presence of similar effectors with a redundant function or a quantitative effect that adds to the

overall virulence arsenal of the fungus.

Compared to other well studied CDIPs, which possess strong activity and trigger death of tobacco leaves within less than 5 days (Ma *et al.*, 2015; Zhang *et al.*, 2017; Zhu *et al.*, 2017; Yang et al., 2018; Bi *et al.*, 2021; Yang *et al.*, 2021; Yin *et al.*, 2021), treatment of leaves with purified BcPTP1 protein or transient expression of using agroinfiltration, both induced chlorosis rather than instant cell death (Fig. 1; Fig. 4A). Hence, the BcPTP1 protein probably does not cause direct damage to the plant cell but more likely, it affects some unknown pathways that eventually lead to cell death, such as accumulation of toxic metabolites or inhibition of photosynthesis.

Homologues of BcPTP1 were found in several additional fungal species, mostly necrotrophic and hemibiotrophic plant pathogens (Supplementary Fig. S2). Significantly, no homologues are found in biotrophic plant pathogens or in human pathogens, which hint to a specific role of the protein in promoting necrotrophic infection. Homologues were also found in saprophytic *Aspergillus* species that colonize and grow on dead plant residues. While these saprotrophic fungi probably do not need the death-inducing activity of the BcPTP1 homologs during their entire life cycle, it is possible that they benefit from an unknown activity of these proteins, or they might have a yet unidentified plant associated phase.

Many effectors contain multiple cysteine residues, which form disulphide bonds (Sevier and Kaiser, 2002; Lu and Edwards, 2016). These residues play significant roles in protein folding, structural stability and protection of such proteins against degradation in harsh acidic and protease-rich environment when they are delivered into plant apoplast during infection (Rep, 2005). BcPTP1 contains 10 cysteine residues that are predicted to form potential disulphide bonds. Mutation of seven out of the 10 cysteine residues in BcPTP1 completely abolished, and an additional one greatly reduced, the phytotoxic activity, whereas mutation of two other residues enhanced the activity (Fig. 5A). It is possible that the majority of the cysteine residues are involved in forming the proper tertiary structure of BcPTP1, thus changing these cysteine residues abolished or decreased the death-inducing activity. The other two residues might be part of epitopes that contribute to the cell death-inducing activity and the mutations might lead to exposure of the immunogenic epitopes, resulting in enhanced activity. Similar study recently revealed that the secreted apoplastic protein PC2 from the potato late blight pathogen *Phytophthora infestans* was cleavage by plant apoplastic proteases, which is the essential process for PC2 to release the immunogenic peptides, thus to activate plant defense responses (Wang *et al.*, 2021a). Indeed, several studies demonstrated that heat denaturation or structural mutation of some secreted proteins did not abolished the necrosis-inducing activity (Zhang *et al.*, 2014a; Zhang *et al.*, 2014b), indicating that the potential epitopes are sufficient for the plant cell death-inducing activity. Similarly, our study also showed that

heat-denatured BcPTP1 still retained a weak cytotoxic activity (Fig. 6). Accordingly, it is possible that in addition to tertiary structure, the unknown immunogenic peptide also contributes to the cell death inducing activity of BcPTP1.

Our study showed that BcPTP1 activates an immune response in *N. benthamiana* as measured by infection assay and induced expression of defense genes (Fig. 8). Thus, the BcPTP1 may also function as a potential elicitor. Indeed, our results demonstrated that BcPTP1 is secreted extracellularly (Fig. 1; Fig. 2) and may interact with plants receptor-like kinases (RLKs) and/or receptor like proteins (RLPs) and transmit signals via the RLKs BAK1 and/or SOBIR1, as other well-known elicitors (Albert *et al.*, 2015; Du *et al.*, 2015; Postma *et al.*, 2016; Franco-Orozco *et al.*, 2017; Zhu *et al.*, 2017; Nie *et al.*, 2019; Nie *et al.*, 2021). However, silencing of *BAK1* or *SOBIR1* in tobacco did not block cell death development but instead, it resulted in induction of more severe and faster plant cell death (Fig. 9). Similar studies had also been reported that some apoplast elicitors could induce necrosis independent of BAK1 and/or SOBIR1, such as BcPG3 (Zhang *et al.*, 2014b), TvEIX (Bar *et al.*, 2010), VdEIX3 (Yin *et al.*, 2021) and Fg12 (Yang *et al.*, 2021). It is possible that BcPTP1 and its putative interacting RLP may coordinate with other unknown LRR-RLKs as co-receptors to transmit immune or death-inducing signals.

Subcellular localization analysis of BcPTP1 showed that the fluorescence signal of BcPTP1-GFP fusion protein is mainly observed in plant cell cytoplasmic vesicles and periphery of plasma membrane, but not the expected apoplastic localization (Fig. 3). This intracellular localization of BcPTP1 is unexpected given that an extracellular localization of the protein is necessary for the cytotoxic activity. Several studies showed that the internalization of certain secreted fungal proteins was dependent on the plasma membrane RLKs BAK1 and/or SOBIR1 (Robatzek, 2006a, Robatzek *et al.*, 2006b; Chinchilla *et al.*, 2007a, Chinchilla *et al.*, 2007b; Liebrand *et al.*, 2013; Wang *et al.*, 2021b). Based on these studies and our findings, we proposed hypothetical model (Fig. 10) in which following secretion by the fungus, the BcPTP1 interacts in the apoplast with a plant RLK and/or RLP, and this complex transmits the phytotoxicity and defense signals. In parallel, the BcPTP1 protein might be also recognized by other plasma membrane receptor that cooperate with the BAK1 and SOBIR1 complex to mediate the internalization through cytoplasmic vesicles (Fig. 10). According to this model, silencing of the *BAK1* or *SOBIR1* genes blocks BcPTP1internalization leading to accumulation of large amounts of BcPTP1 in apoplastic space and increased phytotoxicity.

Acknowledgements

This research was supported by the National Natural Science Foundation of China (Grant No 31972215, 31861143043 and 81903782), Institute of Plant

Protection and Soil Science, Hubei Academy of Agricultural Sciences/Key Laboratory of Integrated Pest Management on Crops in Central China, Ministry of Agriculture, P.R. China/Hubei Key Laboratory of Crop Diseases, Insect Pests and Weeds Control (Grant No 2018ZTSJJ14), and Hubei Province Agricultural Science and Technology Innovation Center Project (Grant No 2018-620-003-001).

Author contributions

WZ and WW: conceptualization of experiments and research plans; WZ, MY, QG, LG and WW: performing the experiments; RX, KB, CX and ZL: data and statistical analysis; WZ, AS, DJ and MW: funding acquisition; AS and WC: manuscript revision; WZ and WW: writing.

Data availability

Data of this study are all available within the paper and within its supplementary data published online. Further information may be obtained from the corresponding author.

Materials and methods

Fungi, bacteria, plants and culture conditions

The *Botrytis cinerea* wild type strain B05.10 and derived transformants used in this study were grown and maintained on PDA medium (Acumedia, MI, USA) at 22□ under continuous fluorescent light supplemented with near-UV (black) light. Conidia of all *B. cinerea* strains were obtained from 7-days-old cultures. *Escherichia coli* strains Rosetta-gami (DE3) and JM109 (Shanghai Weidi Biotechnology, Shanghai, China) were respectively used for proteins expression and plasmid construction. *Agrobacterium tumefaciens* strain GV3101(pSoup) (Shanghai Weidi Biotechnology, Shanghai, China) was used for *Agrobacterium*-mediated transient expression of target proteins in plant leaves.

Tobacco (*Nicotiana benthamiana*), bean (*Phaseolus vulgaris*, genotype N9059), maize (*Zea m*ays cv. Silver Queen) and tomato (*Solanum lycopersicum* cv. Hawaii 7981) plants were grown in a greenhouse under 16-h/8-h intervals of 25°C/22°C, light/dark. *Arabidopsis thaliana* Columbia-0 was grown in a chamber under 16-h/8-h intervals of 22°C/20°C, light/dark.

Plasmid construction

The *bcptp1* gene deletion construct *Del-bcptp1* was generated as described previously (Zhu *et al.*, 2017) that the 5’ (510 bp) and 3’ (516 bp) flanks fragments of *bcptp1* gene were amplified and respectively cloned into the upstream and downstream regions of *hph* cassette using Gibson Assembly Master Mix kit (New

England Biolabs, Massachusetts, USA). The overexpression plasmid OEBcPTP1-pH2G was generated that the full-length open reading frame of *bcptp1* was cloned into the pH2G vector under the regulation of *B. cinerea* histone H2B promoter (NCBI identifier CP009806.1) and the endo-β-1,4-glucanase precursor terminator (NCBI identifier CP009807.1), as described previously (Zhu *et al.*, 2017).

To transiently express the target protein in plant using agroinfiltration, the indicated sequences were cloned into binary plasmid pCNG between the 2×CaMV 35S promoter and NOS terminator (Yang *et al.*, 2018), then transformed into *A. tumefaciens* strain GV3101. The *E. coli* protein expression vectors were constructed that the GFP and *BcPTP1* mature sequence without the signal peptide were, respectively, cloned into vector pET-N-GST-PreScission (Beyotime Biotechnology, Shanghai, China), then transformed into *E. coli* strain Rosetta-gami (DE3). All the primers used for plasmid construction were listed in Table S1.

Manipulation of nucleic acids

Total RNA of fungi and plant samples were isolated using RN03-RNApure Kit (Aidlab, Beijing, China), residual DNA was removed using DNase I (Thermo Scientific, MA, USA) according to manufacturers' protocols and stored at –80°C. The first strand cDNA of indicated sample was generated using RevertAid First Strand cDNA Synthesis Kit (Thermo Scientific, MA, USA). The reverse transcription-quantitative PCR (RT-qPCR) was performed to analyze the gene expression profile using SYBR® Green Supermixes (Bio-Rad, CA, USA) and CFX96 Touch Real-Time PCR Detection System (Bio-Rad, CA, USA) according to manufacturer's instructions. The *B. cinerea Bcgpdh* gene and the *N. benthamiana NbEF1α* gene were, respectively, used as endogenous control genes for normalizing the expression levels of target genes as described previously (Zhu *et al.*, 2017). Primers were designed across or flanking an intron (Supplementary Table S1). For each analyzed gene, RT-qPCR assays were repeated at least twice, each repetition with three independent replicates. The genomic DNA of indicated *B. cinerea* strains were isolated using Fungal Genomic DNA Purification Kit (Simgen, Hangzhou, China) according to the manufacturer's protocol.

Bioinformatics analysis

The NCBI (http://www.ncbi.nlm.nih.gov/) database was used to obtain homologous sequences of BcPTP1 from other pathogens using BLASTp analysis. The JGI (http://genome.jgi.doe.gov/Botci1/Botci1.home.html) database of *B. cinerea* was used to characterize *B. cinerea* genomic and transcriptomic sequences. The HMMSCAN (https://www.ebi.ac.uk/Tools/hmmer/search/hmmscan) was used to analyze the protein domain. The SignalP-5.0 Server

(http://www.cbs.dtu.dk/services/SignalP/) was used to predict signal peptide sequence. The Clustal X and MEGA-X programs were used for protein alignments and phylogenetic tree generation with an unrooted neighbor-joining method. The I-TASSER (http://zhanglab.ccmb.med.umich.edu/I-TASSER/) was used to predict 3D structural model.

Transformation, pathogenicity and cell wall stress tolerance assay of *B. cinerea*

Genetic transformation of *B. cinerea* was performed as described previously (Ma *et al.*, 2017). The *bcptp1* gene deletion mutants *ΔBcPTP1-1* and *ΔBcPTP1-2*, overexpression strains OEBcPTP1-1 and OEBcPTP2, were confirmed using PCR and RT-qPCR.

Pathogenicity assays on the primary leaves of 9-days-old bean were performed as previously described (Zhu *et al.*, 2017). Conidia of indicated *B. cinerea* strains were suspended in inoculation medium (Gamborg's B5 medium containing 2% (w/v) glucose and 10 mM KH_2PO_4/K_2HPO_4, pH6.4), the conidia were diluted to 2×10^5 conidia/ml and leaves were inoculated with 7.5 μl of spore suspension. Plants were incubated in a humid chamber at 22°C for 72 h, and the lesion diameter was measured.

To determine the possible effect of BcPTP1 on stress tolerance and cell wall integrity, the indicated strains were inoculated on PDA plates supplemented with 0.5 mg/ml Congo Red, 0.3 mg/ml Calcofluor White, 1 M sorbitol, 1 M NaCl, 20 mM H_2O_2 and 0.02% SDS at 22°C, as described previously (Zhu *et al.*, 2017).

***A. tumefaciens*-mediated transient expression and Western blotting assay**

A. tumefaciens-mediated transient expression in *N. benthamiana* leaves was performed using agroinfiltration method as previously described (Zhu *et al.*, 2017). For extraction of fungal or plant proteins, 0.2 g of tissue was ground to powder in liquid nitrogen, suspended in 1 ml of cold lysis buffer (Beyotime Biotechnology, Shanghai, China), the samples were incubated on ice for 5 min and then centrifuged at 12,000 *g* for 10 min at 4°C, the supernatant containing soluble proteins was collected. The supernatant proteins were then mixed with 5×SDS-PAGE sample buffer (Beyotime Biotechnology, Shanghai, China), denatured by boiling for 10 min at 100°C and then separated by SDS-PAGE electrophoresis and transferred onto PVDF membranes (0.45 μm). Western blotting was analyzed using anti-GFP antibody (Beyotime Biotechnology, Shanghai, China).

Expression and purification of recombinant BcPTP1 protein

Expression of BcPTP1 and GFP recombinant proteins were performed in *E. coli* strain Rosetta-gami (DE3) as described previously (Zhu *et al.*, 2017). Purification of

recombinant proteins was performed using Glutathione Beads 4FF (Smart-Lifesciences, Changzhou, China) according to manufacturer's instructions. The proteins were cleaned using Amicon Ultra-4 Centrifugal Filter Devices (15 ml, 10 kD; Merck Millipore) to remove the elution buffer, dissolved in phosphate-buffered saline (PBS) and stored at –80°C.

Protein infiltration assay and induction of plant resistance by BcPTP1

To test the phytotoxic activity of BcPTP1, leaves were infiltrated with recombinant protein solution. Plants were then kept in chamber at 25°C and photographed at 10- and 15-days after treatment.

To test the of BcPTP1 on plant defense response and sensitivity to infection, *N. benthamiana* leaves were infiltrated with 10 μg/ml protein solution. The infiltrated plants were kept in a greenhouse for 48 h, and then the treated leaves were inoculated with *B. cinerea* and incubated for an additional 48 h, or used for expression analysis of defense-related genes using RT-qPCR.

VIGS in *N. benthamiana*

To test whether BcPTP1-induced plant death is associated with *NbBAK1* or *NbSOBIR1* in tobacco, VIGS was used to silence the expression of *NbBAK1* or *NbSOBIR1* as described previously (Zhu *et al.*, 2017). The plasmid pTRV2 :: *GFP* was used as the control. The expression level of *NbBAK1* or *NbSOBIR1* in gene silenced *N. benthamiana* was determined by RT-qPCR analysis. Then, the *BcPTP1* was expressed using *A. tumefaciens*-mediated transient expression in the leaves of *NbBAK1* or *NbSOBIR1* silenced *N. benthamiana*. The infiltrated plants were then kept in greenhouse at 25°C and the plant death development was photographed at 10 days and 15 days after infiltration.

Subcellular localization analysis

To analyze the subcellular localization of BcPTP1 in plant cells, the BcPTP1-GFP, BcPTP1$^{\Delta SP}$-GFP, GFP and SP^{BcPTP1}-GFP sequences were cloned into binary vector pCNG between the 2×CaMV 35S promoter and NOS terminator, respectively. Transient expression was carried out using agroinfiltration. *N. benthamiana* leaves epidermal cells were harvested 3 days after agroinfiltration and plasmolyzed in 0.75 M sucrose solution, then the samples were imaged under confocal laser scanning microscope (Leica TCS SP8). Excitation wavelength of 488 nm, emission wavelength of 495-510 nm was used to detect GFP, and 650-750 nm was used for chloroplast autofluorescence.

Statistical analysis

OriginPro 2021b (OriginLab Corporation, Northampton, MA, USA) was used for statistical tests. ANOVA (one-way, $P \leq 0.01$) was used to analyze data significance. In all graphs, results were obtained from three to five independent experiments. Asterisks or different letters in the graphs indicate statistical differences at $P \leq 0.01$.

References

1. **Albert I, Böhm H, Albert M, Feiler CE, Imkampe J, Wallmeroth N, Brancato C, Raaymakers TM, Oome S, Zhang H, Krol E, Grefen C, Gust AA, Chai J, Hedrich R, Van den Ackerveken G, Nürnberger T.** 2015. An RLP23–SOBIR1–BAK1 complex mediates NLP-triggered immunity. Nature Plants **1,** 15140.
2. **Albert I, Hua C, Nürnberger T, Pruitt RN, Zhang L.** 2020. Surface sensor systems in plant immunity. Plant Physiology **182**, 1582–1596.
3. **Bar M, Sharfman M, Ron M, Avni A.** 2010. BAK1 is required for the attenuation of ethylene-inducing xylanase (Eix)-induced defense responses by the decoy receptor LeEix1. Plant Journal **63**, 791–800.
4. **Bi K, Scalschi L, Jaiswal N, Mengiste T, Fried R, Sanz AB, Arroyo J, Zhu W, Masrati G, Sharon A.** 2021. The *Botrytis cinerea* Crh1 transglycosylase is a cytoplasmic effector triggering plant cell death and defense response. Nature Communications **12**, 2166.
5. **Brunner F, Rosahl S, Lee J, Rudd JJ, Geiler C, Kauppinen S, Rasmussen G, Scheel D, Nürnberger T.** 2002. Pep-13, a plant defense-inducing pathogen associated pattern from *Phytophthora* transglutaminases. EMBO Journal **21**, 6681–6688.
6. **Chinchilla D, Boller T, Robatzek S.** 2007a. Flagellin signaling in plant immunity. Advances in Experimental Medicine and Biology **598,** 358–371.
7. **Chinchilla D, Zipfel C, Robatzek S, Kemmerling B, Nürnberger T, Jones JD, Felix G, Boller T.** 2007b. A flagellin-induced complex of the receptor FLS2 and BAK1 initiates plant defence. Nature **448,** 497–500.
8. **Cui H, Tsuda K, Parker JE.** 2015. Effector-triggered immunity: from pathogen perception to robust defense. Annual Review of Plant Biology **66**, 487–511.
9. **de Jonge R, van Esse HP, Maruthachalam K, Bolton MD, Santhanam P, Saber MK, Zhang Z, Usami T, Lievens B, Subbarao KV, Thomma BP.** 2012. Tomato immune receptor Ve1 recognizes effector of multiple fungal pathogens uncovered by genome and RNA sequencing. Proceedings of the National Academy of Sciences, USA **109**, 5110–5115.
10. **Dean R, Van Kan JA, Pretorius ZA, Hammond-Kosack KE, Di Pietro A, Spanu PD, Rudd JJ, Dickman M, Kahmann R, Ellis J, Foster GD.** 2012. The

575 Top 10 fungal pathogens in molecular plant pathology. Molecular Plant Pathology
576 **13**, 414–430.
577 11. **Denton-Giles M, McCarthy H, Sehrish T, Dijkwel Y, Mesarich CH,**
578 **Bradshaw RE, Cox MP, Dijkwel PP.** 2020. Conservation and expansion of a
579 necrosis-inducing small secreted protein family from host-variable
580 phytopathogens of the Sclerotiniaceae. Molecular Plant Pathology **21**, 512–526.
581 12. **Du J, Verzaux E, Chaparro-Garcia A, Bijsterbosch G, Keizer LC, Zhou J,**
582 **Liebrand TW, Xie C, Govers F, Robatzek S, van der Vossen EA, Jacobsen E,**
583 **Visser RG, Kamoun S, Vleeshouwers VG.** 2015. Elicitin recognition confers
584 enhanced resistance to *Phytophthora infestans* in potato. Nature Plants **1**, 15034.
585 13. **Eizner E, Ronen M, Gur Y, Gavish A, Zhu W, Sharon A.** 2017.
586 Characterization of *Botrytis*-plant interactions using PathTrack©: an automated
587 system for dynamic analysis of disease development. Molecular Plant Pathology
588 **18**, 503–512.
589 14. **Fliegmann J, Mith□fer A, Wanner G, Ebel J.** 2004. An ancient enzyme domain
590 hidden in the putative β-glucan elicitor receptor of soybean may play an active
591 part in the perception of pathogen-associated molecular patterns during broad host
592 resistance. Journal of Biological Chemistry **279,** 1132–1140.
593 15. **Franco-Orozco B, Berepiki A, Ruiz O, Gamble L, Griffe LL, Wang S, Birch**
594 **PRJ, Kanyuka K, Avrova A**. 2017. A new proteinaceous pathogen-associated
595 molecular pattern (PAMP) identified in Ascomycete fungi induces cell death in
596 Solanaceae. New Phytologist **214**, 1657–1672.
597 16. **Frías M, González C, Brito N**. 2011. BcSpl1, a cerato-platanin family protein,
598 contributes to *Botrytis cinerea* virulence and elicits the hypersensitive response in
599 the host. New Phytologist **192**, 483–495.
600 17. **Frías M, González M, González C, Brito N.** 2016. BcIEB1, a *Botrytis cinerea*
601 secreted protein, elicits a defense response in plants. Plant Science **250,** 115–124.
602 18. **Gao Y, Faris JD, Liu Z, Kim YM, Syme RA, Oliver RP, Xu SS, Friesen TL.**
603 2015. Identification and characterization of the SnTox6-*Snn6* interaction in the
604 *Parastagonospora nodorum*-wheat pathosystem. Molecular Plant-Microbe
605 Interactions **28,** 615–625.
606 19. **Gui YJ, Chen JY, Zhang DD, Li NY, Li TG, Zhang WQ, Wang XY, Short**
607 **DPG, Li L, Guo W, Kong ZQ, Bao YM, Subbarao KV, Dai XF.** 2017.
608 *Verticillium dahliae* manipulates plant immunity by glycoside hydrolase 12
609 proteins in conjunction with carbohydrate-binding module 1. Environmental
610 Microbiology **19,** 1914–1932.
611 20. **Heard S, Brown NA, Hammond-Kosack K.** 2015. An interspecies comparative
612 analysis of the predicted secretomes of the necrotrophic plant pathogens
613 *Sclerotinia sclerotiorum* and *Botrytis cinerea*. PLoS ONE **10,** e0130534.

21. **Jones JDG, Dangl JL.** 2006. The plant immune system. Nature **444,** 323–329.
22. **Kanneganti T, Huitema E, Cakir C, Kamoun S.** 2006. Synergistic interactions of the plant cell death pathways induced by *Phytophthora infestans* Nep1-like protein PiNPP1.1 and INF1 elicitin. Molecular Plant-Microbe Interactions **19,** 854–863.
23. **Kim K-T, Jeon J, Choi J, Cheong K, Song H, Choi G, Kang S, Lee Y-H.** 2016. Kingdom-wide analysis of fungal small secreted proteins (SSPs) reveals their potential role in host association. Frontiers in Plant Science **7,** 186.
24. **Li Y, Han Y, Qu M, Chen J, Chen X, Geng X, Wang Z, Chen S.** 2020. Apoplastic cell death-inducing proteins of filamentous plant pathogens: roles in plant-pathogen interactions. Frontiers in Genetics **11,** 661.
25. **Liebrand TW, van den Berg GC, Zhang Z, Smit P, Cordewener JH, America AH, Sklenar J, Jones AM, Tameling WI, Robatzek S, Thomma BP, Joosten MH.** 2013. Receptor-like kinase SOBIR1/EVR interacts with receptor-like proteins in plant immunity against fungal infection. Proceedings of the National Academy of Sciences, USA **110,** 10010–10015.
26. **Lo Presti L, Lanver D, Schweizer G, Tanaka S, Liang L, Tollot M, Zuccaro A, Reissmann S, Kahmann R.** 2015. Fungal effectors and plant susceptibility. Annual Review of Plant Biology **66,** 513–545.
27. **Lorang J, Kidarsa T, Bradford CS, Gilbert B, Curtis M, Tzeng SC, Maier CS, Wolpert TJ.** 2012. Tricking the guard: exploiting plant defense for disease susceptibility. Science **338,** 659–662.
28. **Lu S, Edwards MC.** 2016. Genome-wide analysis of small secreted cysteine-rich proteins identifies candidate effector proteins potentially involved in *Fusarium graminearum*-wheat interactions. Phytopathology **106,** 166–176.
29. **Ma L, Salas O, Bowler K, Oren-Young L, Bar-Peled M, Sharon A.** 2017. Genetic alteration of UDP-rhamnose metabolism in *Botrytis cinerea* leads to the accumulation of UDP-KDG that adversely affects development and pathogenicity. Molecular Plant Pathology **18,** 263–275.
30. **Ma Z, Song T, Zhu L, Ye W, Wang Y, Shao Y, Dong S, Zhang Z, Dou D, Zheng X, Tyler BM, Wang Y.** 2015. A *Phytophthora sojae* glycoside hydrolase 12 protein is a major virulence factor during soybean infection and is recognized as a PAMP. Plant Cell **27,** 2057–2072.
31. **Ma Z, Zhu L, Song T, Wang Y, Zhang Q, Xia Y, Qiu M, Lin Y, Li H, Kong L, Fang Y, Ye W, Wang Y, Dong S, Zheng X, Tyler BM, Wang Y.** 2017. A paralogous decoy protects *Phytophthora sojae* apoplastic effector PsXEG1 from a host inhibitor. Science **355,** 710–714.
32. **Marianayagam NJ, Sunde M, Matthews JM.** 2004. The power of two: protein dimerization in biology. Trends in Biochemical Sciences **29,** 618–625.

653 33. **Nie J, Yin Z, Li Z, Wu Y, Huang L.** 2019. A small cysteine-rich protein from
654 two kingdoms of microbes is recognized as a novel pathogen-associated molecular
655 pattern. New Phytologist **222,** 995–1011.
656 34. **Nie J, Zhou W, Liu J, Tan N, Zhou JM, Huang L.** 2021. A receptor-like
657 protein from *Nicotiana benthamiana* mediates VmE02 PAMP-triggered immunity.
658 New Phytologist **229,** 2260–2272.
659 35. **Oome S, Raaymakers TM, Cabral A, Samwel S, B□hm H, Albert I,**
660 **Nürnberger T, Van den Ackerveken G.** 2014. Nep1-like proteins from three
661 kingdoms of life act as a microbe-associated molecular pattern in *Arabidopsis*.
662 Proceedings of the National Academy of Sciences, USA **111,** 16955–16960.
663 36. **Postma J, Liebrand TWH, Bi G, Evrard A, Bye RR, Mbengue M, Kuhn H,**
664 **Joosten MHAJ, Robatzek S.** 2016. Avr4 promotes Cf-4 receptor-like protein
665 association with the BAK1/SERK3 receptor-like kinase to initiate receptor
666 endocytosis and plant immunity. New Phytologist **210,** 627–642.
667 37. **Rep M.** 2005. Small proteins of plant-pathogenic fungi secreted during host
668 colonization. FEMS Microbiology Letters **253,** 19–27.
669 38. **Robatzek S.** 2006a. Vesicle trafficking in plant immune responses. Cell
670 Microbiology **9,** 1–8.
671 39. **Robatzek S, Chinchilla D, Boller T.** 2006b. Ligand-induced endocytosis of the
672 pattern recognition receptor FLS2 in *Arabidopsis*. Genes and Development **20,**
673 537–542.
674 40. **Rotblat B, Enshell-Seijffers D, Gershoni JM, Schuster S, Avni A.** 2002.
675 Identification of an essential component of the elicitation active site of the EIX
676 protein elicitor. Plant Journal **32,** 1049–1055.
677 41. **Sevier CS, Kaiser CA.** 2002. Formation and transfer of disulphide bonds in
678 living cells. Nature Reviews Molecular Cell Biology **3,** 836–847.
679 42. **Shao D, Smith DL, Kabbage M, Roth MG.** 2021. Effectors of plant
680 necrotrophic fungi. Frontiers in Plant Science **12,** 687713.
681 43. **Shinya T, Nakagawa T, Kaku H, Shibuya N.** 2015. Chitin-mediated
682 plant–fungal interactions: catching, hiding and handshaking. Current Opinion in
683 Plant Biology **26,** 64–71.
684 44. **Stergiopoulos I, de Wit PJGM.** 2009. Fungal effector proteins. Annual Review
685 of Phytopathology **47,** 233–263.
686 45. **Thomma BP, Nürnberger T, Joosten MH.** 2011. Of PAMPs and effectors: the
687 blurred PTI-ETI dichotomy. Plant Cell **23,** 4–15.
688 46. **van Ooijen G, van den Burg HA, Cornelissen BJ, Takken FL.** 2007. Structure
689 and function of resistance proteins in solanaceous plants. Annual Review of
690 Phytopathology **45,** 43–72.
691 47. **Veloso J, van Kan JAL.** 2018. Many shades of grey in *Botrytis*-host plant

692 interactions. Trends in Plant Science **23,** 613–622.
693 48. **Wang D, Chen J-Y, Song J, Li J-J, Klosterman SJ, Li R, Kong Z-Q,**
694 **Subbarao KV, Dai X-F, Zhang D-D.** 2021b. Cytotoxic function of xylanase
695 VdXyn4 in the plant vascular wilt pathogen *Verticillium dahliae*. Plant Physiology
696 https://doi.org/10.1093/plphys/kiab274
697 49. **Wang Y, Xu Y, Sun Y, Wang H, Qi J, Wan B, Ye W, Lin Y, Shao Y, Dong S,**
698 **Tyler BM, Wang Y.** 2018. Leucine-rich repeat receptor-like gene screen reveals
699 that *Nicotiana* RXEG1 regulates glycoside hydrolase 12 MAMP detection. Nature
700 Communications **9,** e594.
701 50. **Wang S, Xing R, Wang Y, Shu H, Fu S, Huang J, Paulus JK, Schuster M,**
702 **Saunders DGO, Win J, Vleeshouwers V, Wang Y, Zheng X, van der Hoorn**
703 **RAL, Dong S.** 2021a. Cleavage of a pathogen apoplastic protein by plant
704 subtilases activates host immunity. New Phytologist **229,** 3424–3439.
705 51. **Yang B, Wang Y, Tian M, Dai K, Zheng W, Liu Z, Yang S, Liu X, Shi D,**
706 **Zhang H, Wang Y, Ye W, Wang Y.** 2021. Fg12 ribonuclease secretion
707 contributes to *Fusarium graminearum* virulence and induces plant cell death.
708 Journal of Integrative Plant Biology **63,** 365–377.
709 52. **Yang G, Tang L, Gong Y, Xie J, Fu Y, Jiang D, Li G, Collinge DB, Chen W,**
710 **Cheng J.** 2018. A cerato-platanin protein SsCP1 targets plant PR1 and contributes
711 to virulence of *Sclerotinia sclerotiorum*. New Phytologist **217,** 739–755.
712 53. **Yin Z, Wang N, Pi L, Li L, Duan W, Wang X, Dou D.** 2021. *Nicotiana*
713 *benthamiana* LRR-RLP NbEIX2 mediates the perception of an EIX-like protein
714 from *Verticillium dahliae*. Journal of Integrative Plant Biology **63,** 949–960.
715 54. **Zhang H, Wu Q, Cao S, Zhao T, Chen L, Zhuang P, Zhou X, Gao Z.** 2014a. A
716 novel protein elicitor (SsCut) from *Sclerotinia sclerotiorum* induces multiple
717 defense responses in plants. Plant Molecular Biology **86,** 495–511.
718 55. **Zhang L, Kars I, Essenstam B, Liebrand TWH, Wagemakers L, Elberse J,**
719 **Tagkalaki P, Tjoitang D, van den Ackerveken G, van Kan JAL.** 2014b.
720 Fungal endopolygalacturonases are recognized as microbe-associated molecular
721 patterns by the *Arabidopsis* receptor-like protein RESPONSIVENESS TO
722 BOTRYTIS POLYGALACTURONASES1. Plant Physiology **164,** 352–364.
723 56. **Zhang L, Ni H, Du X, Wang S, Ma XW, Nürnberger T, Guo HS, Hua C.** 2017.
724 The *Verticillium*-specific protein VdSCP7 localizes to the plant nucleus and
725 modulates immunity to fungal infections. New Phytologist **215,** 368–381.
726 57. **Zhu W, Ronen M, Gur Y, Minz-Dub A, Masrati G, Ben-Tal N, Sharon I,**
727 **Savidor A, Eizner E, Valerius O, Braus G, Bowler K, Bar-Peled M, Sharon A.**
728 2017. BcXYG1, a secreted xyloglucanase from *Botrytis cinerea*, triggers both cell
729 death and plant immune responses. Plant Physiology **175,** 438–456.
730

Figure legends

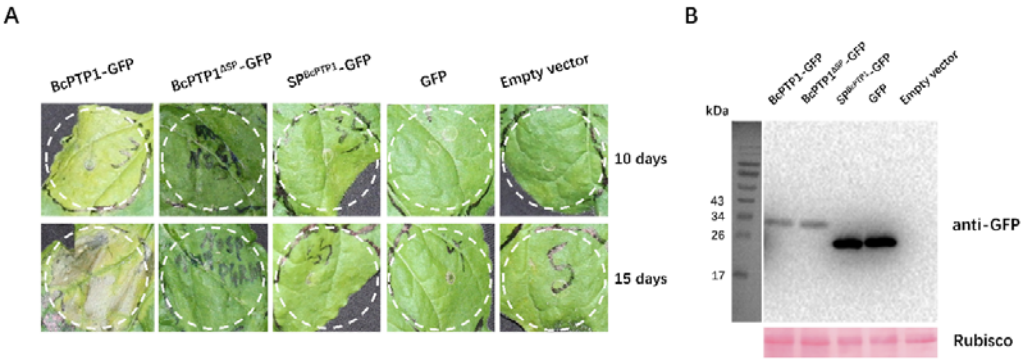

Fig. 1. BcPTP1 is a phytotoxic secreted protein. (A) Images of *N. benthamiana* leaves 10 days and 15 days after agroinfiltration with *A. tumefaciens* strains carrying the indicated constructs. The *A. tumefaciens* carrying the empty vector was used as control. BcPTP1-GFP, BcPTP1 fused with GFP at the C-terminus; $BcPTP1^{\Delta SP}$-GFP, BcPTP1 without signal peptide fused with GFP at the C-terminus; SP^{BcPTP1}-GFP, GFP fused with the signal peptide of BcPTP1. (B) Immunoblot analysis of proteins from *N. benthamiana* leaves transiently expressing the indicated constructs. Top panel, immunoblot using anti-GFP antibody; bottom panel, staining of the Rubisco large subunit with Ponceau S.

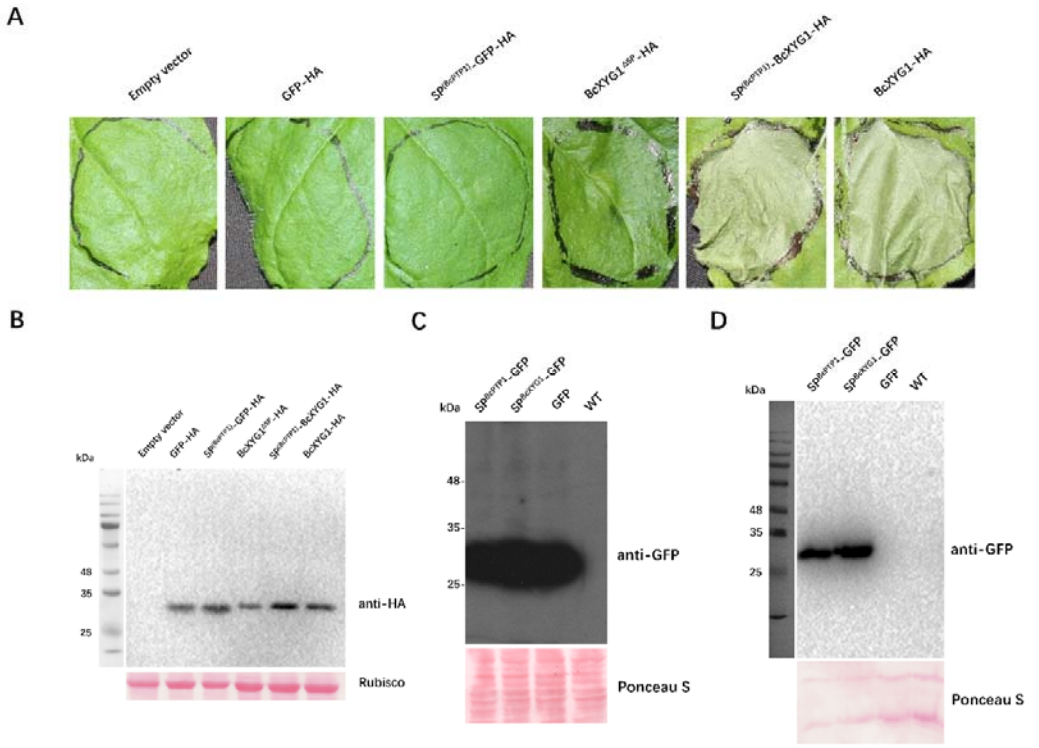

Fig. 2. BcPTP1 signal peptide possesses secretion function. (A) Images of *N. benthamiana* leaves 5 days after agroinfiltration with *A. tumefaciens* strains carrying the indicated constructs. The *A. tumefaciens* carrying the empty vector was used as control. GFP-HA, HA-tagged GFP; $SP^{(BcPTP1)}$-GFP-HA, HA-tagged GFP with the signal peptide of BcPTP1; $BcXYG1^{\Delta SP}$-HA, HA-tagged BcXYG1 lacking the native signal peptide; $SP^{(BcPTP1)}$-BcXYG1-HA, HA-tagged BcXYG1 with its native signal peptide replaced with the BcPTP1 signal peptide; BcXYG1-HA, HA-tagged BcXYG1 with its native signal peptide. (B) Immunoblot analysis of proteins from *N. benthamiana* leaves transiently expressing the indicated constructs. Top panel, immunoblot using anti-HA antibody; bottom panel, staining of the Rubisco large subunit with Ponceau S. (C-D) The indicated genes were expressed under the regulation of *B. cinerea* histone H2B promoter (NCBI identifier CP009806.1) and the endo-β-1,4-glucanase precursor terminator (NCBI identifier CP009807.1). The *B. cinerea* strains were cultured in PDB medium for 72 h, then the culture filtrate was collected and purified by filtration. (C) Immunoblot analysis of total mycelia proteins from indicated *B. cinerea* strains. Top panel, immunoblot using anti-GFP antibody; bottom panel, Ponceau S staining of the total mycelia proteins. (D) Immunoblot analysis of culture filtrate proteins from indicated *B. cinerea* strains. Top panel, immunoblot using anti-GFP antibody; bottom panel, Ponceau S staining of the secretory proteins. SP^{BcPTP1}-GFP, GFP fused with the signal peptide of BcPTP1; SP^{BcXYG1}-GFP, GFP fused with the signal peptide of BcXYG1; GFP, GFP

780 overexpression strain; WT, wild type strain.

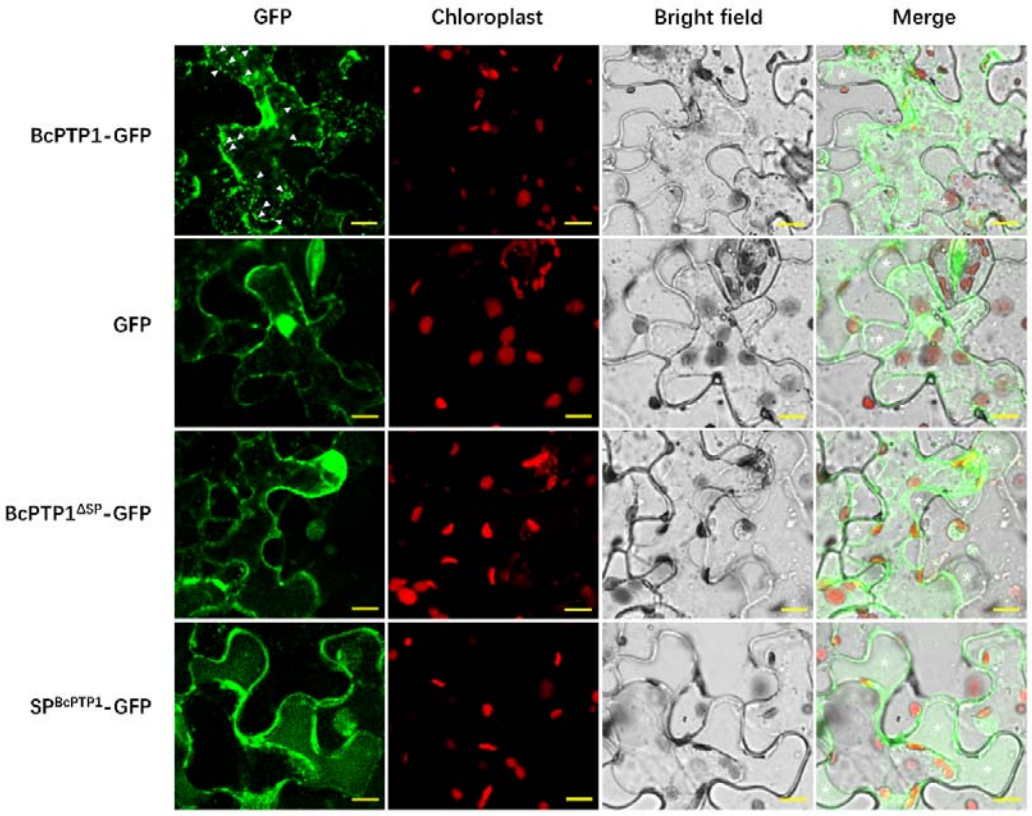

781

782

783 **Fig. 3. Subcellular localization of BcPTP1 in *N. benthamiana* epidermal cells.**
784 Leaves epidermal cells were harvested 3 days after agroinfiltration and plasmolyzed
785 in 0.75 M sucrose solution, then the samples were scanned by confocal laser scanning
786 microscope. BcPTP1-GFP, GFP fused to full length BcPTP1; BcPTP1$^{\Delta SP}$-GFP, GFP
787 fused to BcPTP1 without signal peptide; SP^{BcPTP1}-GFP, GFP fused to the BcPTP1
788 signal peptide. The white arrows indicate the internalized cytoplasmic vesicle. White
789 asterisks mark apoplastic space of plant cells. Bars = 10 μm.

790

791

792

793

794

795

796

797

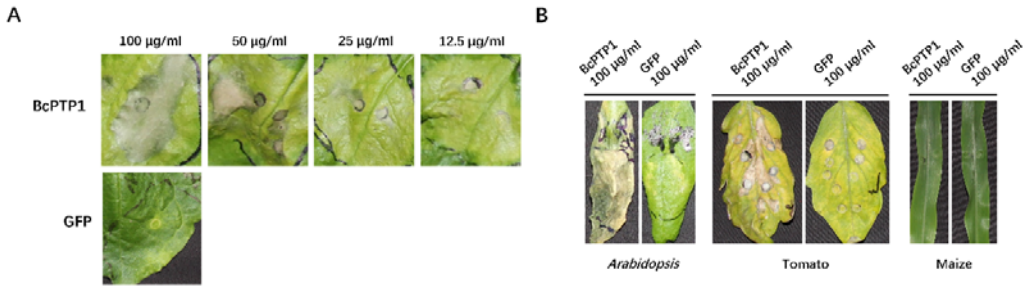

Fig. 4. The BcPTP1 protein is phytotoxic to dicot but not monocot plant species. Proteins were produced in *E. coli*, purified and suspended in phosphate-buffered saline (PBS). (A) Response of *N. benthamiana* leaves infiltrated with different concentrations of BcPTP1 at 15 days after treatment. (B) Response of Arabidopsis, tomato and maize leaves infiltrated with 100 µg/ml protein solution.

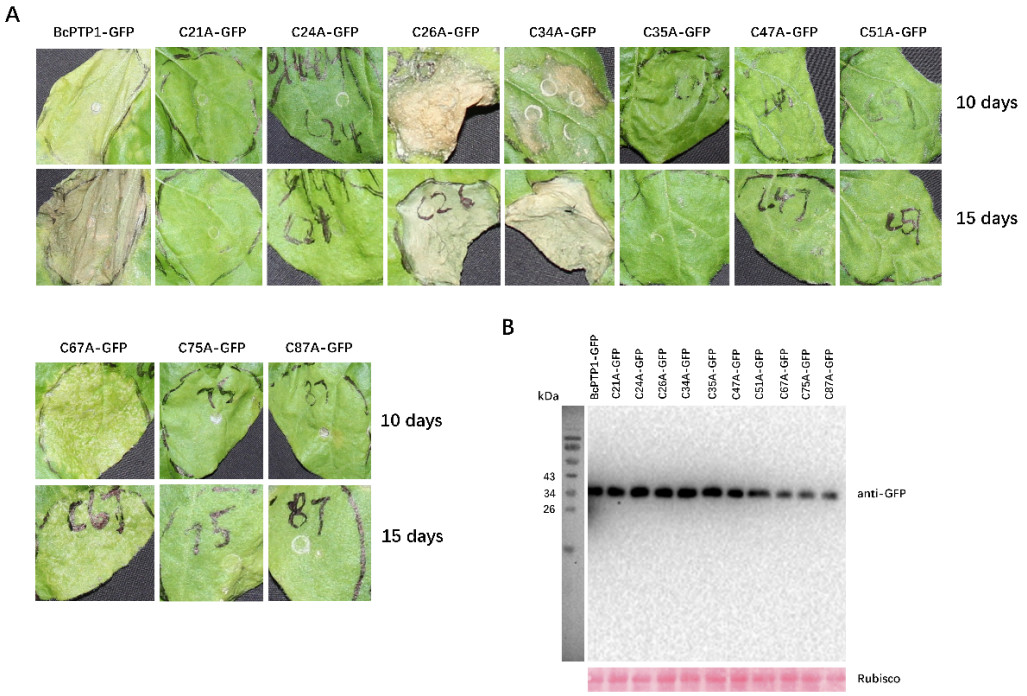

Fig. 5. Specific cysteine residues necessary for BcPTP1 phytotoxicity. (A) Images of *N. benthamiana* leaves 10 days and 15 days after transient agroinfiltration. (B) Immunoblot analysis of proteins from *N. benthamiana* leaves transiently expressing the cysteine residue mutant constructs. Top panel, immunoblot using anti-GFP antibody; Bottom panel, staining of the Rubisco large subunit with Ponceau S.

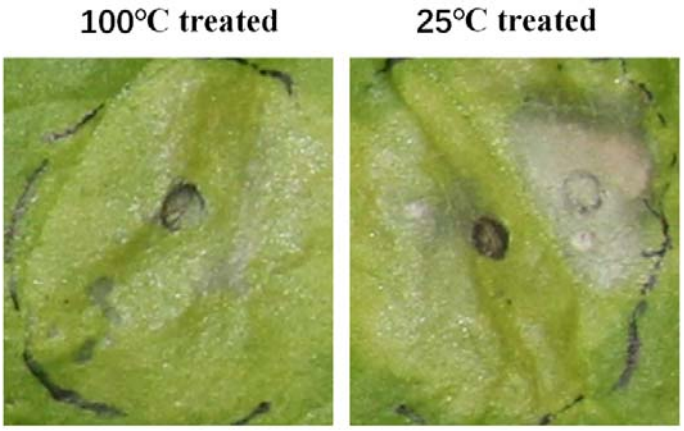

Fig. 6. Phytotoxicity of BcPTP1 is partially heat-stable. Images of *N. benthamiana* leaves 15 days after infiltration with 50 µg/ml of heat-treated (100□ treated for 30 min) and native (25□ treated for 30 min) BcPTP1 protein.

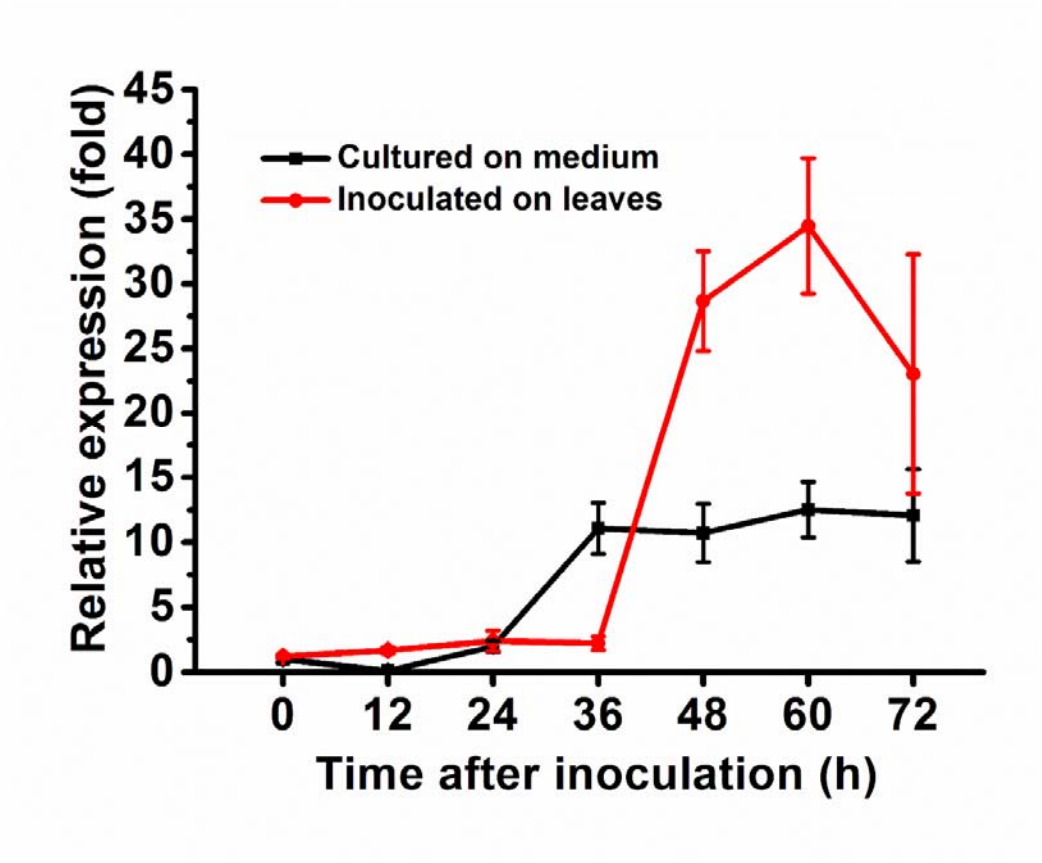

Fig. 7. Expression of the *BcPTP1* gene is up-regulated at late infection stage. Bean leaves (red line) or Gamborg's B5 medium (black line) were inoculated with *B. cinerea* conidia, and expression levels of the *BcPTP1* gene were evaluated by RT-qPCR. The expression level of *BcPTP1* inoculated on plant or in Gamborg's B5 medium at 0 h was set as 1, and relative transcript levels were calculated using the comparative Ct method. Transcript levels of the *B. cinerea Bcgpdh* gene were used to normalize different samples. Data represent means and standard deviations of three independent replications.

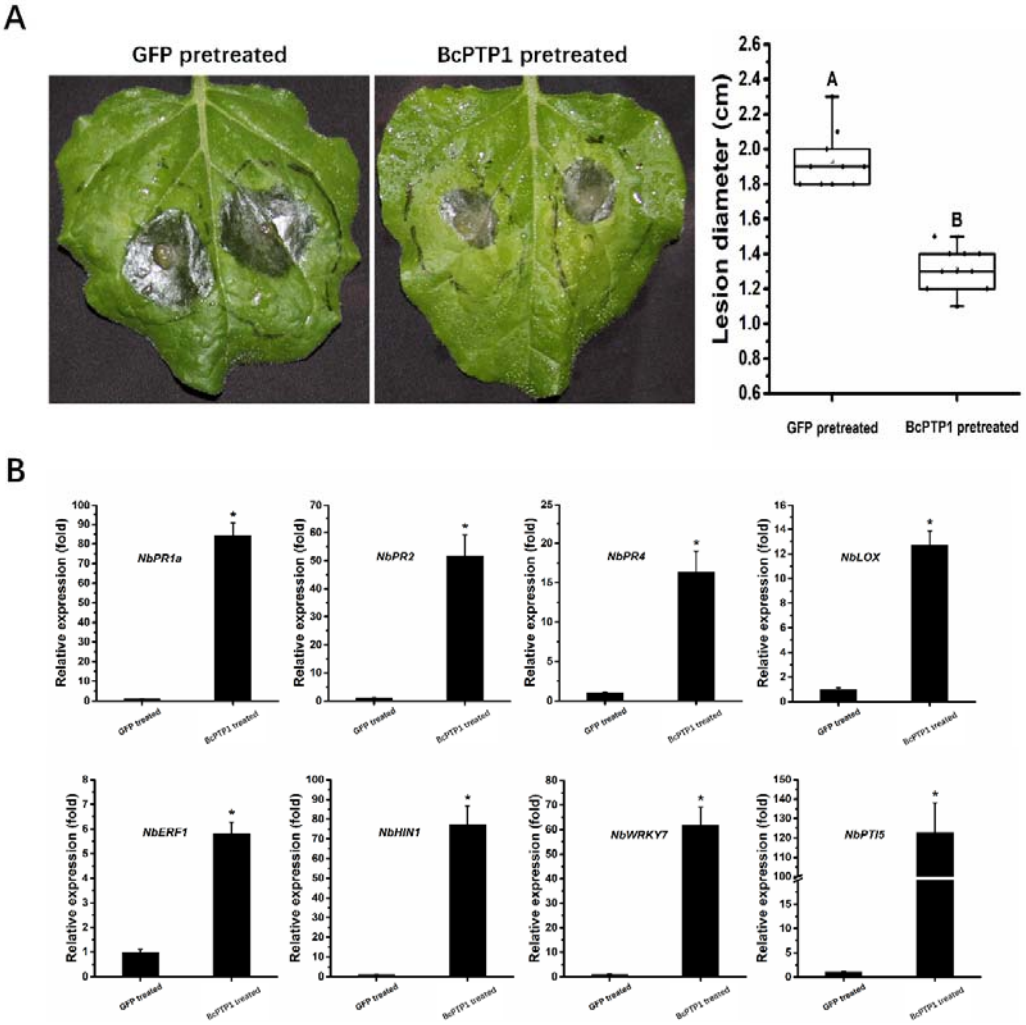

Fig. 8. BcPTP1 induces resistance in tobacco. (A) *N. benthamiana* leaves were infiltrated with 10 μg/ml purified BcPTP1 or GFP protein. After 2 days, the infiltrated leaves were inoculated with *B. cinerea* in a humid chamber. The lesions were photographed and measured at 48 hpi. Data were obtained from three independent experiments with total 10 samples. In box plots, whiskers indicate the minimum and maximum values, the line indicates the median, the box boundaries indicate the upper (25th percentile) and lower (75th percentile) quartiles, all data are plotted as black dots. Different letters in the graph indicate statistical differences at $P \leq 0.01$ using ANOVA (one-way). (B) Relative expression levels of defense-related genes from *tobacco* leaves that treated with BcPTP1 or GFP for 48 h were determined by RT-qPCR analysis. The expression level of indicated genes in GFP-treated leaves were set as 1. The expression level of the tobacco *NbEF1α* gene was used to normalize different samples. Data represent means and standard deviations of three independent replicates. Asterisks in the graph indicate statistical differences at $P \leq$

903 0.01 using ANOVA (one-way).

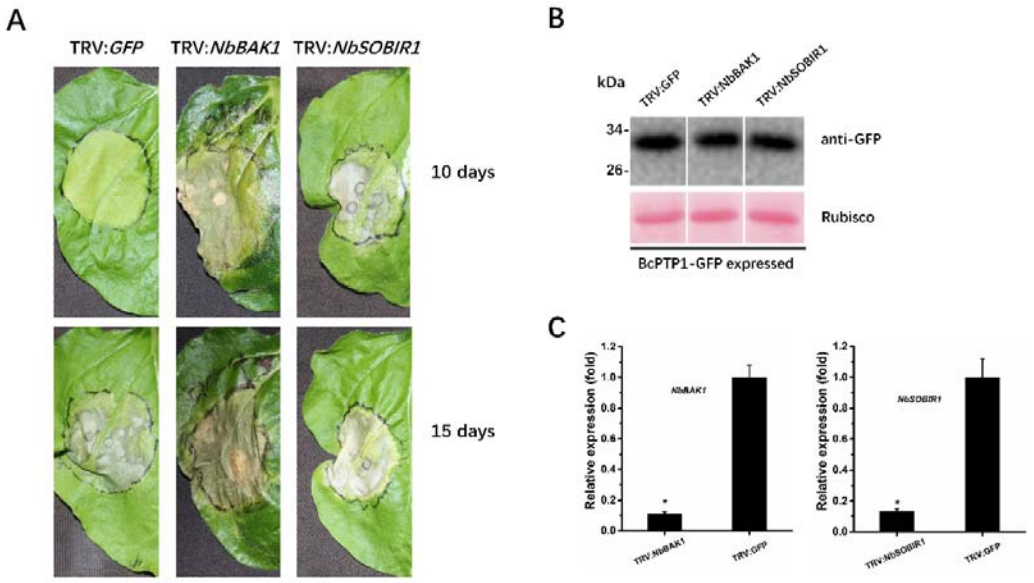

904

905 **Fig. 9. BAK1 and SOBIR1 negatively regulate the death-inducing activity of**
906 **BcPTP1 in *N. benthamiana.*** TRV-based VIGS vectors were used to initiate silencing
907 of *NbBAK1* (TRV : *NbBAK1*) and *NbSOBIR1* (TRV : *NbSOBIR1*). TRV : *GFP* was
908 used as a control virus treatment in these experiments. (A) Three weeks after initiation
909 of VIGS, *BcPTP1-GFP* was transiently expressed in the gene-silenced leaves using
910 agroinfiltration. Leaves were photographed 10 and 15 days after treatment. (B)
911 Immunoblot analysis of proteins from indicated *N. benthamiana* leaves transiently
912 expressing BcPTP1-GFP. Top panel: BcPTP1-GFP was detected using anti-GFP
913 antibody; bottom panel, staining of the Rubisco large subunit with Ponceau S. (C)
914 *NbBAK1* and *NbSOBIR1* expression levels in gene-silenced tobacco leaves were
915 determined by RT-qPCR analysis. Expression level in control plants (TRV : *GFP*) was
916 set as 1. *NbEF1α* was used as an endogenous control. Data represent means and
917 standard deviations from three biological replicates. Asterisks indicate significant
918 differences ($P \leq 0.01$).

919

920

921

922

923

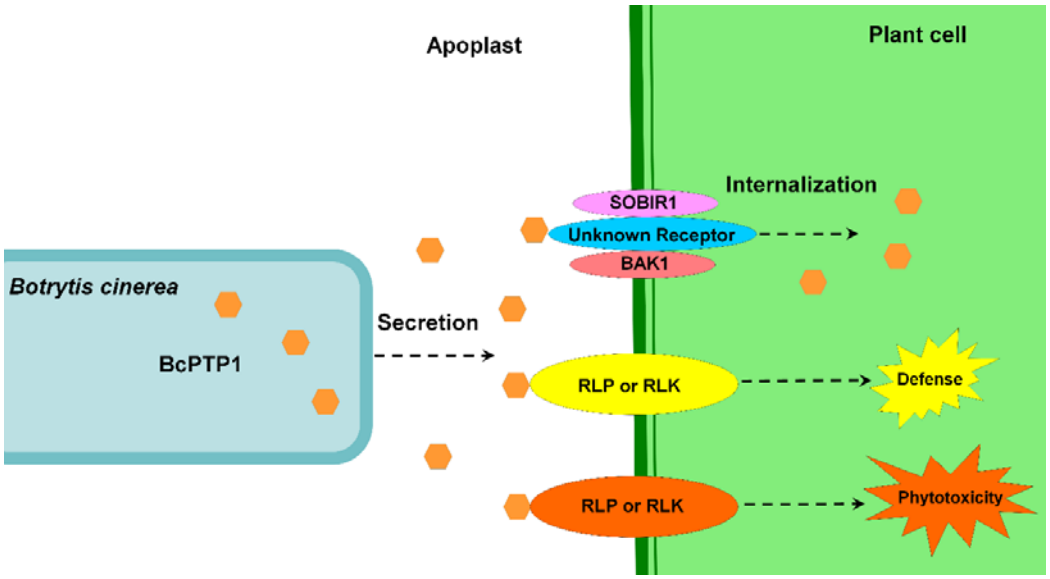

Fig. 10. The model illustrating the internalization of BcPTP1 mediated by BAK1 and SOBIR1, and the defense and phytotoxicity induced by BcPTP1 though RLPs or PLKs in plant cell. BcPTP1 is secreted from *B. cinerea* hyphae into apoplastic space to interact with plants RLKs and/or RLPs and transmit the phytotoxicity and defense signals. BcPTP1 can also be recognized by other unknown receptor that cooperate with BAK1 and SOBIR1 complex to mediate the internalization.

946

947

948 # Supplemental data

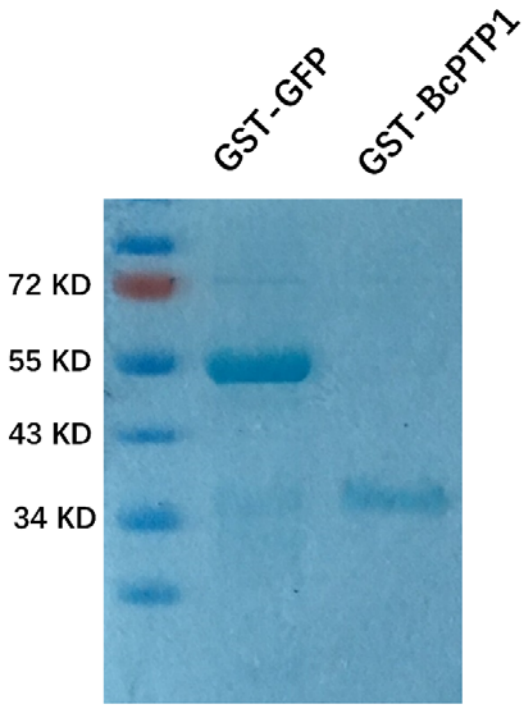

949

950 **Fig. S1. Expression of recombinant proteins.** SDS-PAGE analysis of purified GST-
951 BcPTP1 and GST-GFP proteins from *E. coli* stained with Coomassie Blue.

952

953

954

955

956

957

958

959

960

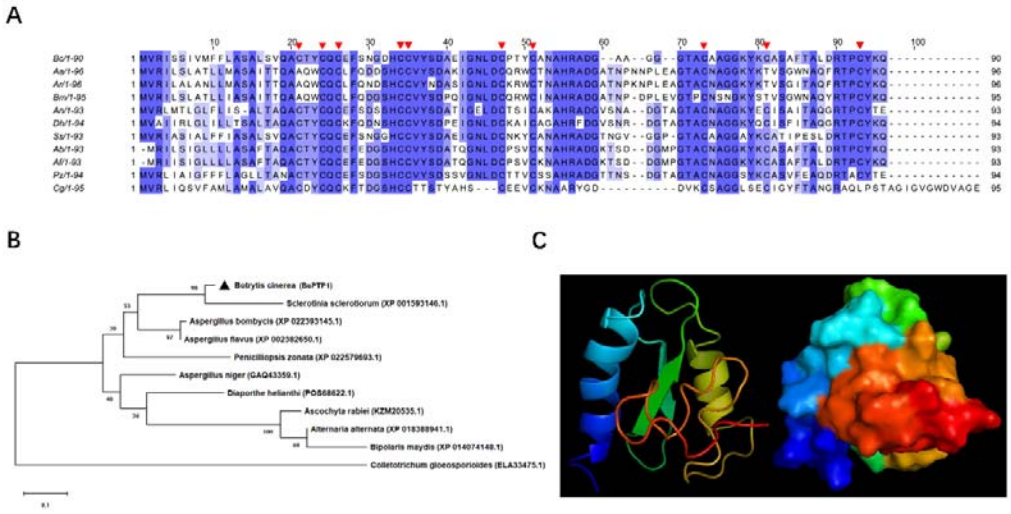

Fig. S2. Sequence similarities between BcPTP1 and its homologs. (A) Multiple sequence alignment of BcPTP1 and its homologs. Full-length protein sequences were aligned using *Clustal W* and the alignment was edited using *Jalview*. The red triangles show the cysteine residues. Intensity of blue shading reflects the level of amino acid identity at each position. Bc: *B. cinerea* BcPTP1 (BCIN_05g03680); Ss: *S. sclerotiorum* (XP_001593146.1, E-value: 8e-45, 80% identity); Ab: *Aspergillus bombycis* (XP_022393145.1, E-value: 2e-39, 72% identity); Af: *A. flavus* (XP_002382650.1, E-value: 2e-39, 72% identity); Aa: *A. alternata* (XP_018388941.1, E-value: 1e-31, 58% identity); An: *A. niger* (GAQ43359.1, E-value: 2e-31, 61% identity); Cg: *C. gloeosporioide*s (ELA33475.1, E-value: 4e-09, 44% identity); Pz: *Penicilliopsis zonata* (XP_022579693.1, E-value: 5e-34, 63% identity); Ar: *Ascochyta rabiei* (KZM20535.1, E-value: 2e-31, 58% identity); Dh: *Diaporthe helianthi* (POS68622.1, E-value: 4e-31, 61% identity); Bm: *Bipolaris maydis* (XP_014074148.1, E-value: 2e-29, 55% identity). (B) Phylogenetic analysis of BcPTP1 and its homologs from other fungi. The full-length protein sequences were analyzed using *MEGA X* with Unrooted neighbor-joining bootstrap (1,000 replicates). The black triangle mark location of BcPTP1. A scale bar at the lower left corresponds to a genetic distance of 0.1. (C) 3D structural models of BcPTP1, predicted using *I-TASSER* and further analyzed by *PyMOL* software. Left: cartoon models; right: surface models.

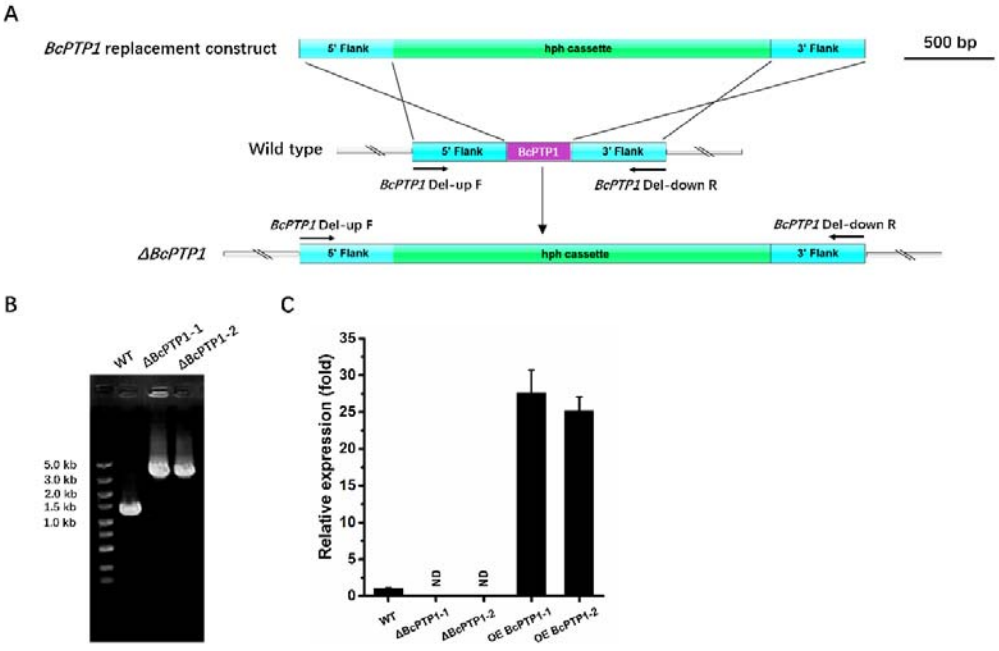

Fig. S3. The *bcptp1* gene deletion strategy and confirmation in *B. cinerea*. (A) Strategy used to generate the *bcptp1* gene deletion mutants. The deletion construct used to transform the wild type strain contained the hygromycin resistance (*hph*) cassette flanked by upstream and downstream sequence of the *bcptp1* gene. The positions of the PCR primers used to verify the deletion transformants are indicated (*BcPTP1* Del-up F and *BcPTP1* Del-down R). The scale bar indicates 500 bp. (B) PCR amplifications carried out to verify the *bcptp1* deletion mutants using the 5' flank For and 3' flank Rev primers. As templates, genomic DNA from either the wild type strain or the *bcptp1* deletion mutants Δ*BcPTP1*-1 and Δ*BcPTP1*-2, was used as indicated. (C) RT-qPCR carried out to analyze the expression levels of the *bcptp1* gene in the wild type strain, the *bcptp1* deletion mutants Δ*BcPTP1*-1 and Δ*BcPTP1*-2, the *bcptp1* overexpression strains OE *BcPTP1*-1 and OE *BcPTP1*-2. The strains cultured on PDA at 22°C for 72 h were used for RT-qPCR analysis. The relative levels of transcript were calculated using the comparative Ct method. The *bcptp1* gene expression level in wild type strain was set as level 1. The transcript level of the *B. cinerea bcgpdh* gene was used to normalize different samples. Data represent means and standard deviations of three independent replicates. ND=not detected.

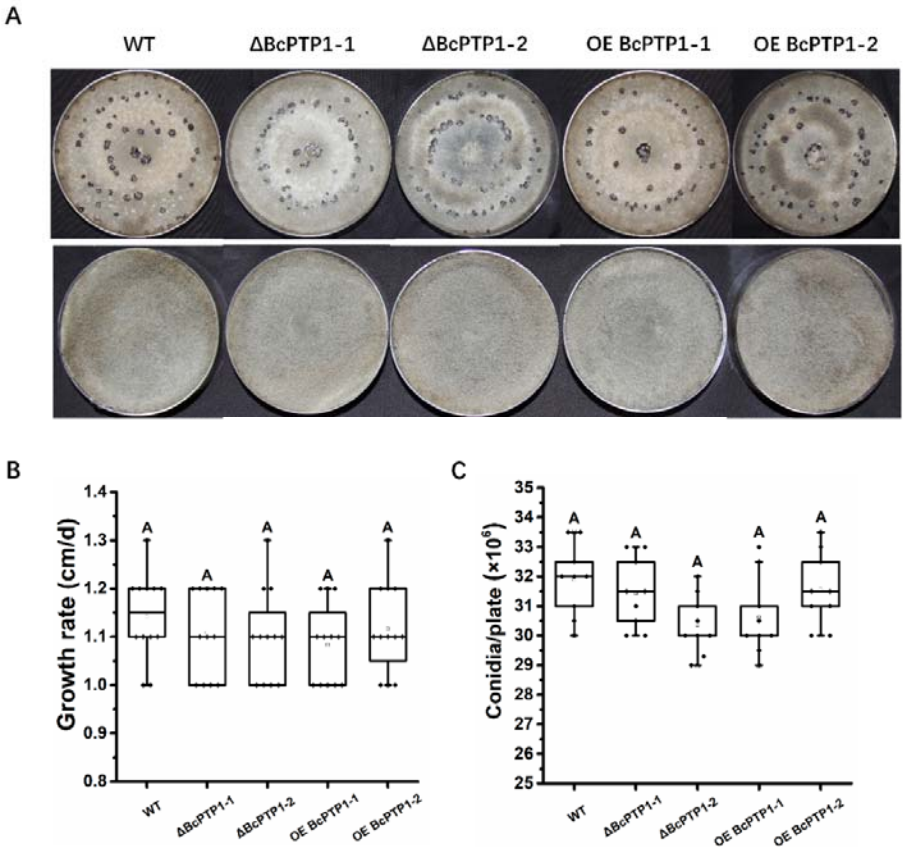

Fig. S4. Phenotypes of *B. cinerea* wild type, and the *bcptp1* deletion and overexpression strains. (A) Colony morphology, sporulation and sclerotia formation. Top: colonies on PDA at 22°C for 15 days in complete darkness. Bottom: *B. cinerea* strains on PDA plates at 22°C for 7 days with continuous fluorescent light. (B) Hyphal growth rate. *B. cinerea* strains were grown on PDA plates at 22°C with continuous fluorescent light. Radial growth was measured every day for 5 days and growth rate was calculated. Data were obtained from three independent experiments, with four replicates in each experiment. In box plots, whiskers indicate the minimum and maximum values, the line indicates the median, the box boundaries indicate the upper (25th percentile) and lower (75th percentile) quartiles, all data are plotted as black dots. Same letters in the graph indicate no statistical differences at $P \leq 0.01$ using one-way ANOVA one-way. (C) Conidial production of indicated strains cultured on PDA plates at 22 °C for 7 days. Conidiation of each strain was determined by collecting and counting conidia with a hematocytometer. Data were obtained from three independent experiments, with three replicates in each experiment. In box plots, whiskers indicate the minimum and maximum values, the line indicates the median, the box boundaries indicate the upper (25th percentile) and lower (75th percentile) quartiles, all data are plotted as black dots. Same letters in the graph indicate no statistical differences at $P \leq 0.01$ using one-way ANOVA.

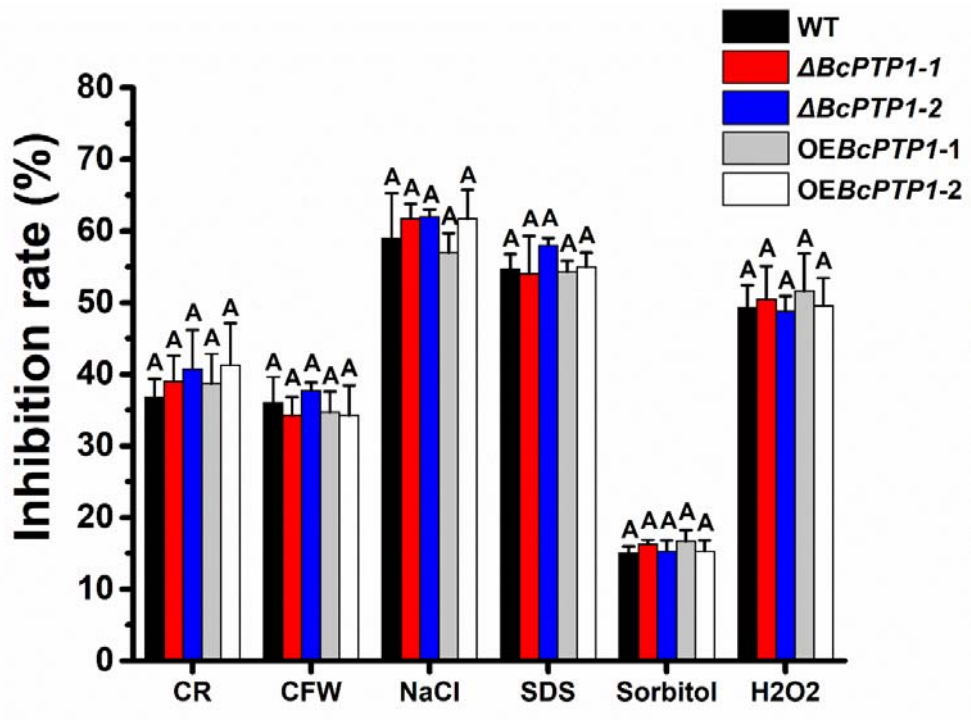

Fig. S5. *bcptp1* deletion does not affect stress tolerance of *B. cinerea*. Inhibition rate of the radial growth of wild type strain, *bcptp1* deletion mutants and *bcptp1* overexpression strains were analyzed on PDA plates supplemented with 0.5 mg/ml Congo Red, 0.3 mg/ml Calcofluor White, 1 M sorbitol, 1 M NaCl, 20 mM H_2O_2 and 0.02% SDS at 22°C, respectively. Data represent means and standard deviations from three independent experiments, each with three replications. Same letters in the graph indicate no statistical differences at $P \leq 0.01$ using ANOVA (one-way).

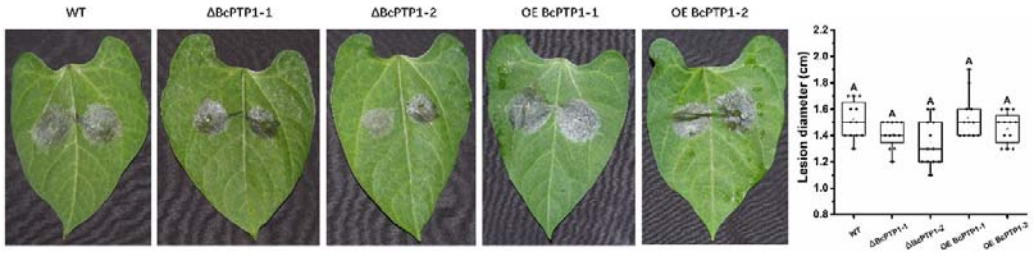

Fig. S6. Pathogenicity analysis of *B. cinerea* strains. Beans leaves were inoculated with 7.5 µl of conidia suspension (2×10^5 conidia/ml). The plants were incubated in a humid chamber at 22°C for 72 h, photographed and lesion size was determined. Data were obtained from three independent experiments, with four replicates in each experiment. In box plots, whiskers indicate the minimum and maximum values, the line indicates the median, the box boundaries indicate the upper (25th percentile) and lower (75th percentile) quartiles, all data are plotted as black dots. Same letters in the graph indicate no statistical differences at $P \leq 0.01$ using ANOVA (one-way).

1088 **Table S1. Primers used for vector construction and PCR.**

Primer purpose	Primer name and sequence
bcptp1 deletion for upstream	*BcPTP1* Del-up F: 5' TGTTGGGTCTTATGCGGAAAGAGAC 3'
	BcPTP1 Del-up R: 5'CCTTTTTTTTTCAGGAATTATTCTCACAGTTTTGACGGTAGTGAAAAGGACTTTG 3'
bcptp1 deletion for downstream	BcPTP1 Del-down F: 5'GATCTAGATGCATTCGCGAGGTACCGAGCTGAATCTCCGATGGGATGGAGAGTTCT 3'
	BcPTP1 Del-down R: 5' ATCGATGGCTTGTTGTTCATCTTC 3'
bcptp1 over expression	*BcPTP1*-OE F: 5' GGCGCGCCATGGTCCGCATCTCCTCCAT 3'
	BcPTP1-OE R: 5' GCGGCCGCTTACTGCTTGTAACATGGGGTACGATC 3'
bcptp1 transient expression	*BcPTP1*-TE R: 5' TCTAGAATGGTCCGCATCTCCTCCAT 3'
	BcPTP1-TE R: 5' CCCGGGCTGCTTGTAACATGGGGTACGATC 3'
bcptp1$^{\Delta SP}$ transient expression	*BcPTP1*$^{\Delta SP}$-TE R: 5' TCTAGAATGTGCACCTATTGCCAGTGCG 3'
	BcPTP1$^{\Delta SP}$-TE R: 5' CCCGGGCTGCTTGTAACATGGGGTACGATC 3'
GFP transient expression	*GFP*-TE F: 5' TCTAGAATGGTGAGCAAGGGCGAGGAG 3'
	GFP-TE R: 5' GAGCTCTTACTTGTACAGCTCGTCCATGCCG 3'
hph cassette	*hph* cassette F: 5' AGCTCGGTACCTCGCGAATGCATCTAGATC 3'
	hph cassette R: 5' ACTGTGAGAATAATTCCTGAAAAAAAAAGG 3'
bcptp1 for RT-qPCR	*BcPTP1*-q F: 5' TCACTGCTGTGTCTATTCGGATG 3'
	BcPTP1-q R: 5' CGCACTTGTATTTTCCTCCAGC 3'
bcgpdh for RT-qPCR	*Bcgpdh*-q F: 5'CGAAGAATAGCACAAACAGCTGGAC 3'
	Bcgpdh-q R: 5'CGTCACCTTATGCTTCTTGCTCC 3'
GFP expression in *E. coli*	*GFP* GST F: 5' CATATGGTGAGCAAGGGCGAGGAG 3'
	GFP GST R: 5' CTCGAGTTACTTGTACAGCTCGTCCATGCCG 3'

BcPTP1 expression in *E. coli*	*BcPTP1* GST F: 5' CATATGTGCACCTATTGCCAGTGCG 3'
	BcPTP1 GST R: 5'CTCGAGTTACTGCTTGTAACATGGGGTACGATC 3'
NbBAK1 for RT-qPCR	*NbBAK1*-q F: 5'GAGGTGGGAGGAATGGCAAA 3'
	NbBAK1-q R: 5'TTGGCCCCGACAATTCATCT 3'
NbSOBIR1 for RT-qPCR	*NbSOBIR1*-q F: 5'CCAGCAAGTCACAGAAGGGA 3'
	NbSOBIR1-q R: 5'CCAACACCACACCAAAGCTG 3'
NbPR1a for RT-qPCR	*NbPR1a-q* F: 5' CCGCCTTCCCTCAACTCAAC 3'
	NbPR1a-q R: 5' GCACAACCAAGACGTACTGAG 3'
NbPR2 for RT-qPCR	*NbPR2-q* F: 5' AGGTGTTTGCTATGGAATGC 3'
	NbPR2-q R: 5' TCTGTACCCACCATCTTGC 3'
NbPR4 for RT-qPCR	*NbPR4-q* F: 5' GGCCAAGATTCCTGTGGTAGAT 3'
	NbPR4-q R: 5' CACTGTTGTTTGAGTTCCTGTTCCT 3'
NbLOX for RT-qPCR	*NbLOX-q* F: 5' AAAACCTATGCCTCAAGAAC 3'
	NbLOX-q R: 5' ACTGCTGCATAGGCTTTGG 3'
NbERF1 for RT-qPCR	*NbERF1-q* F: 5' GCTCTTAACGTCGGATGGTC 3'
	NbERF1-q R: 5' AGCCAAACCCTAGCTCCATT 3'
NbHIN1 for RT-qPCR	*NbHIN1-q* F: 5' CCAACTTGAACGGAGCCTATTA 3'
	NbHIN1-q R: 5' AGGCATCCAAAGAGACAACTAC 3'
NbWRKY7 for RT-qPCR	*NbWRKY7-q* F: 5' CACAAGGGTACAAACAACACAG 3'
	NbWRKY7-q R: 5' GGTTGCATTTGGTTCATGTAAG 3'
NbPTI5 for RT-qPCR	*NbPTI5-q* F: 5' CCTCCAAGTTTGAGCTCGGATAGT 3'
	NbPTI5-q R: 5' CCAAGAAATTCTCCATGCACTCTGTC 3'
NbEF1α for RT-qPCR	*NbEF1α*-q F: 5' TGGACACAGGGACTTCATCA 3'
	NbEF1α-q R: 5' CAAGGGTGAAAGCAAGCAAT 3'

A

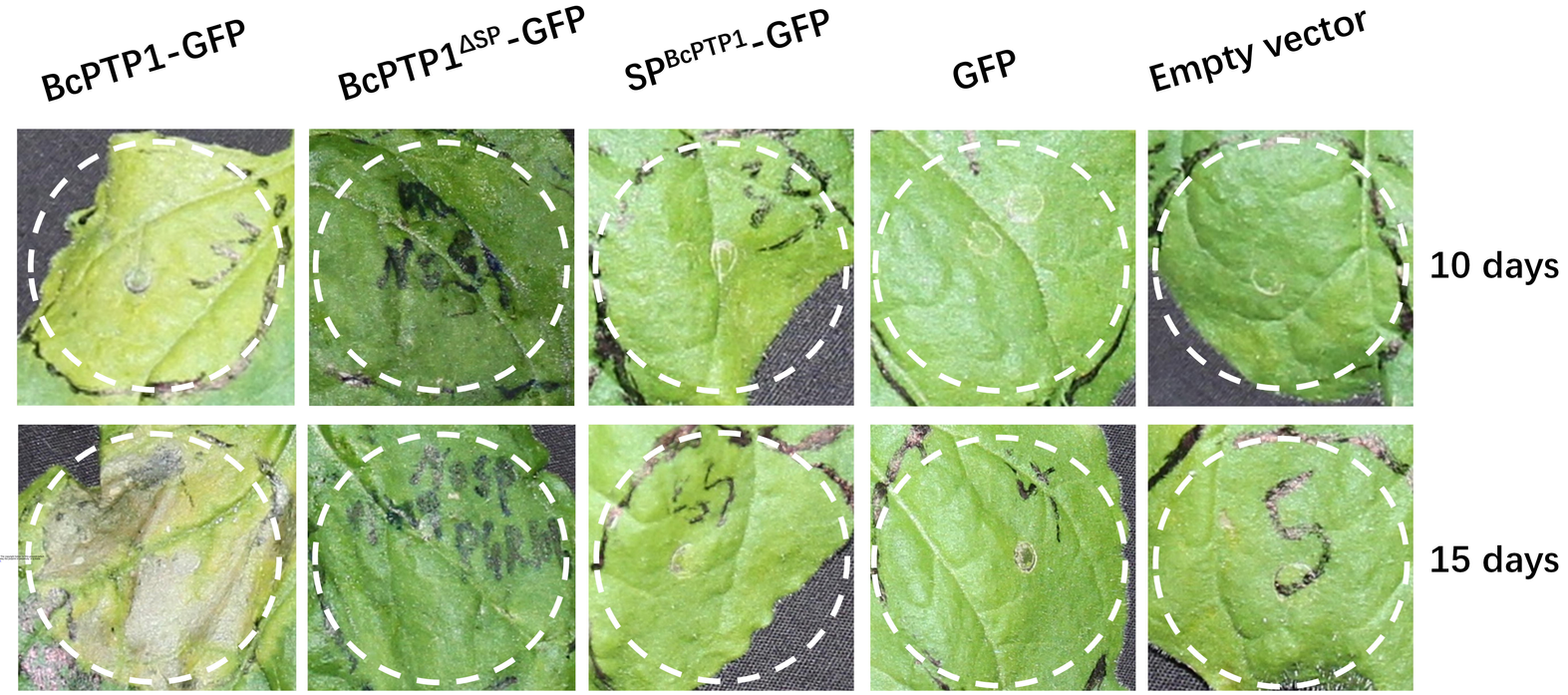
BcPTP1-GFP
BcPTP1ΔSP-GFP
SPBcPTP1-GFP
GFP
Empty vector
10 days
15 days

B

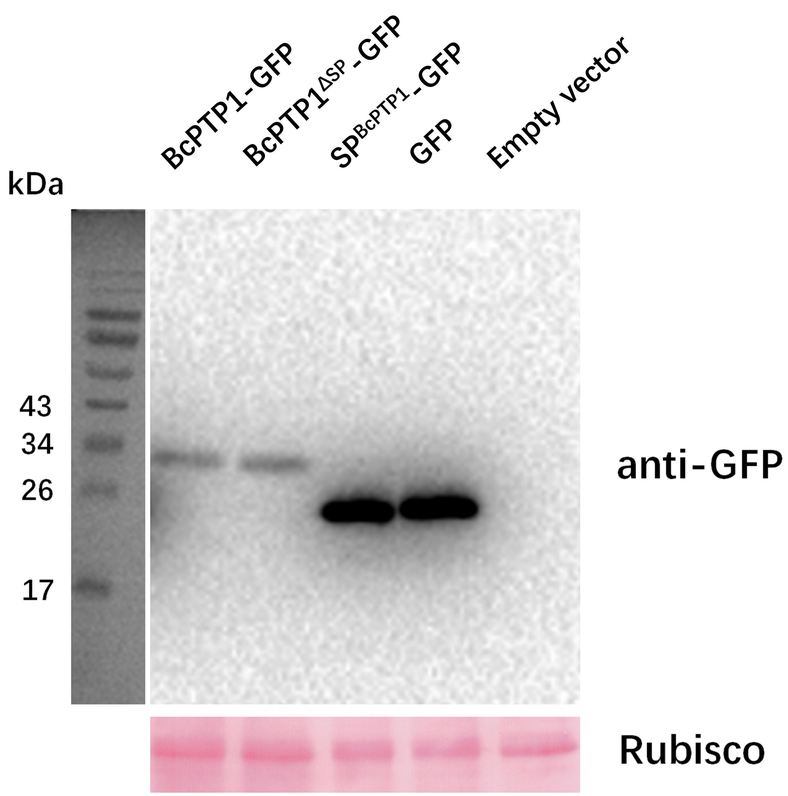
BcPTP1-GFP
BcPTP1ΔSP-GFP
SPBcPTP1-GFP
GFP
Empty vector
kDa
43
34
26
17
anti-GFP
Rubisco

A

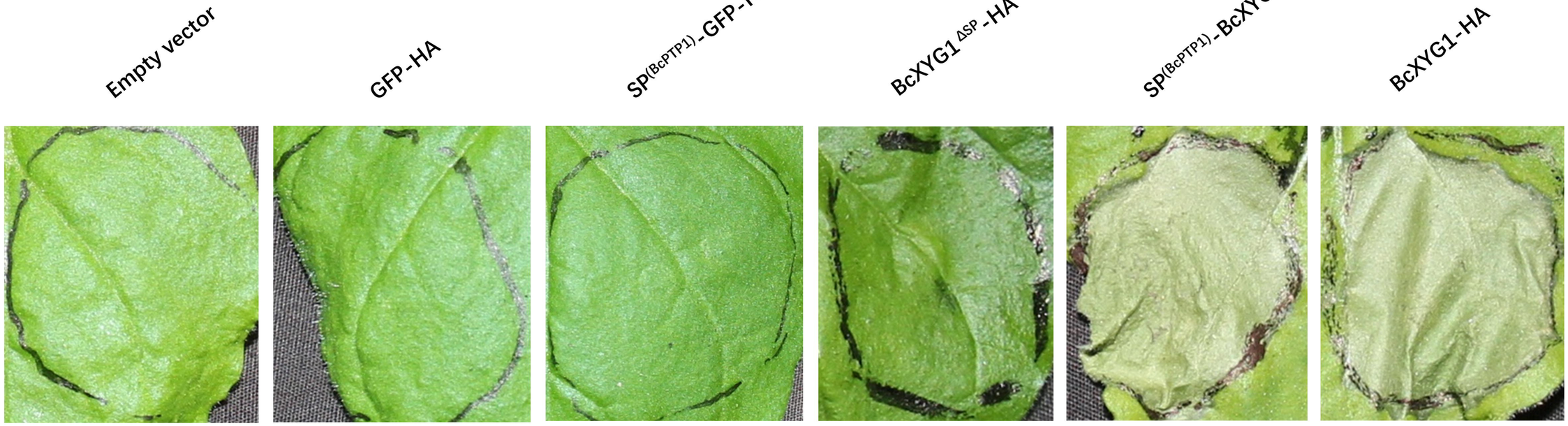

B

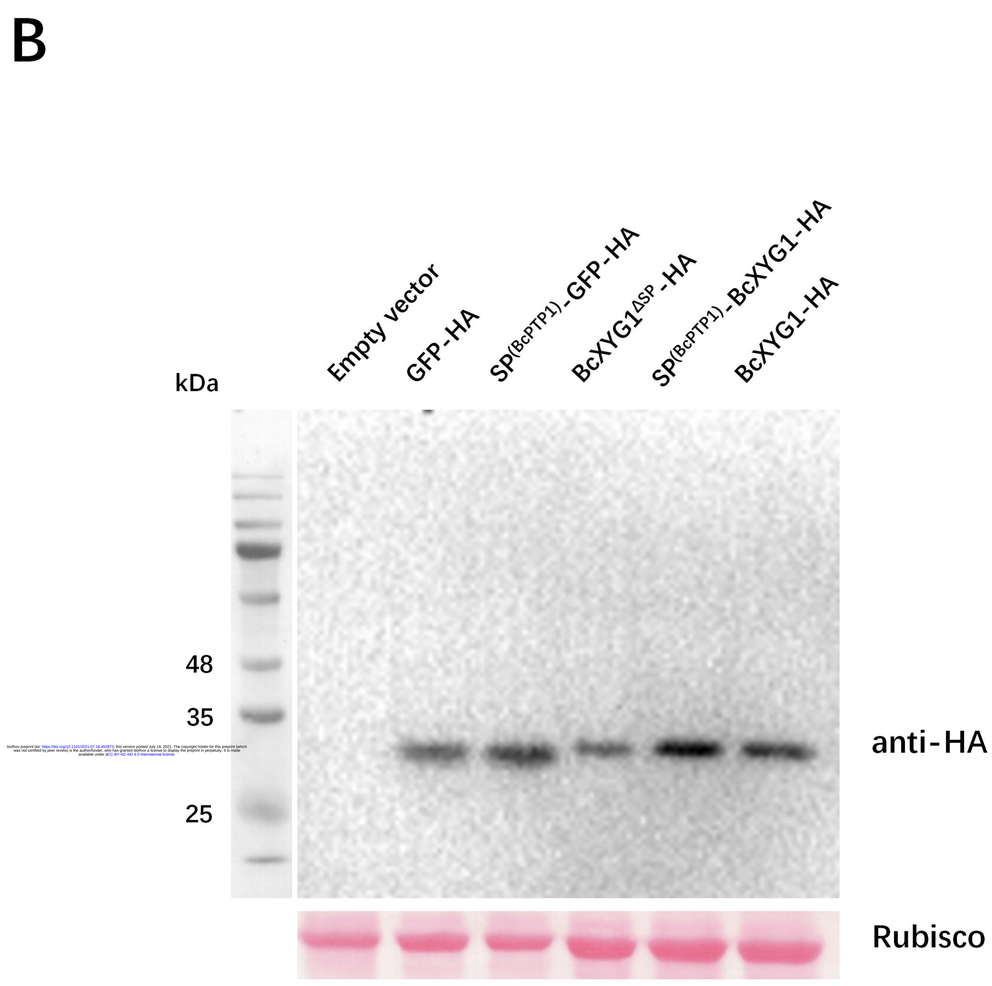

C

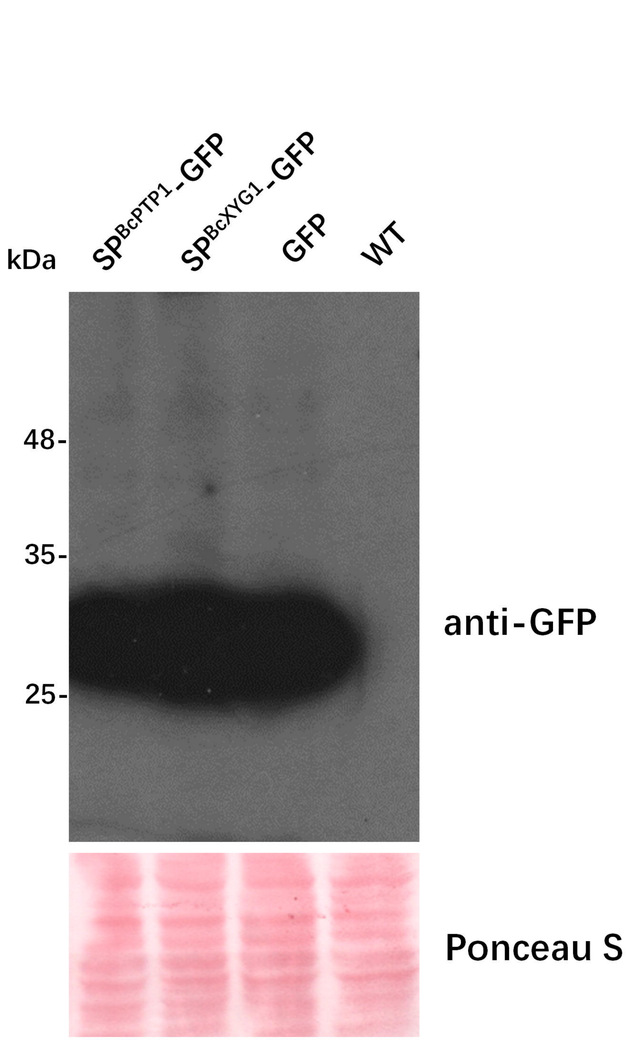

D

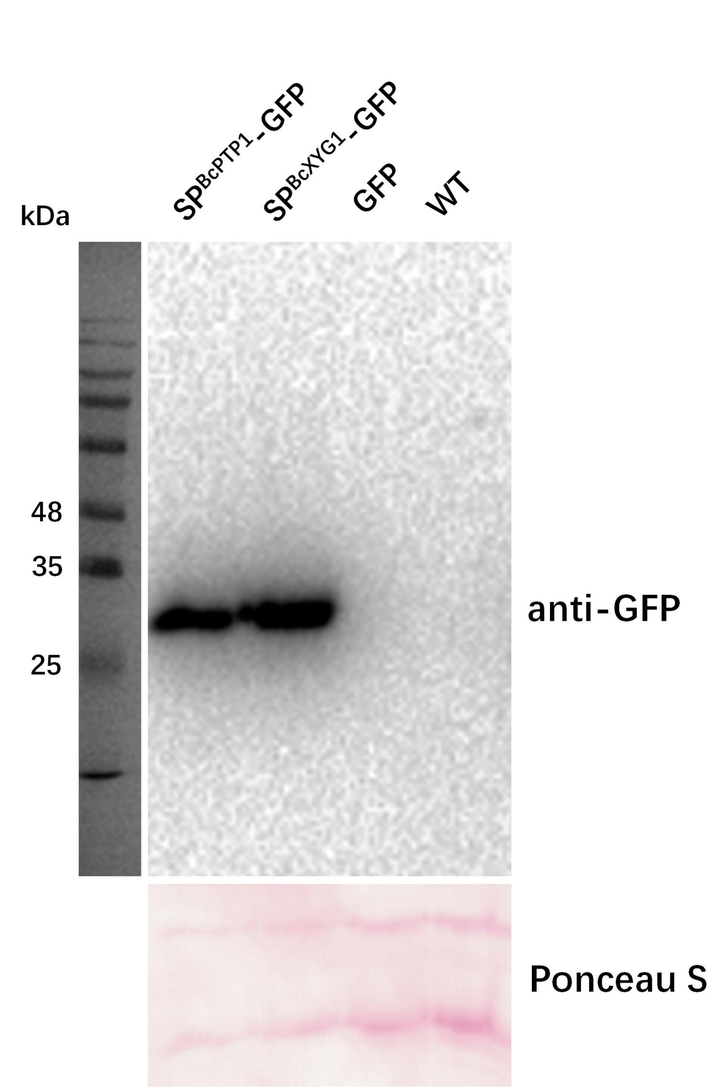

GFP | Chloroplast | Bright field | Merge

BcPTP1-GFP

GFP

$BcPTP1^{\Delta SP}$-GFP

SP^{BcPTP1}-GFP

A

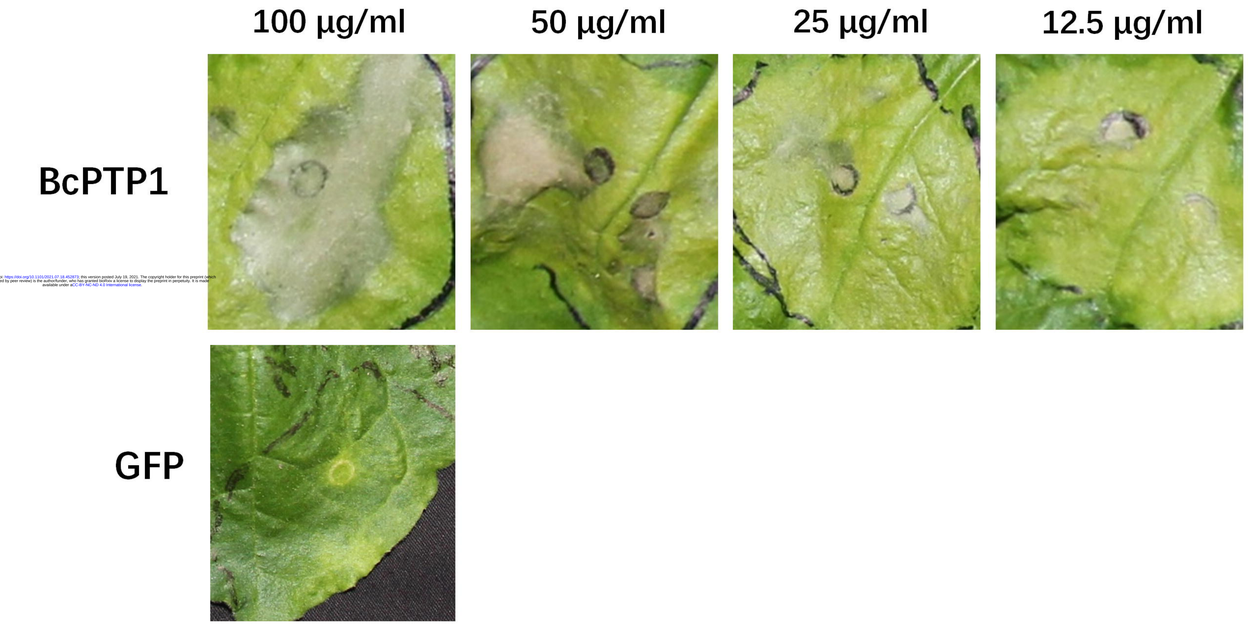

B

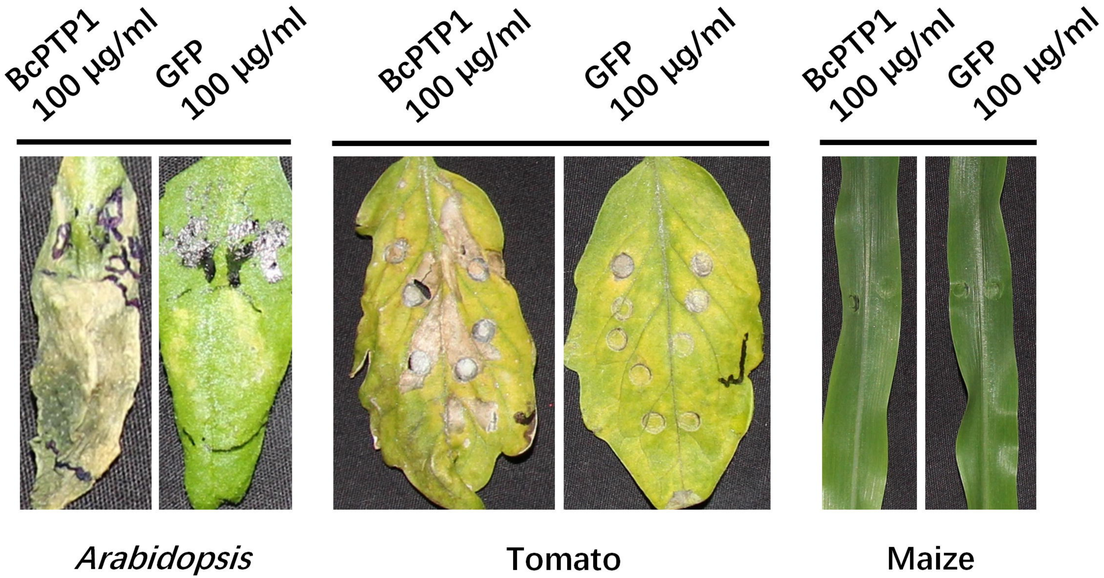

A


BcPTP1-GFP
C21A-GFP
C24A-GFP
C26A-GFP
C34A-GFP
C35A-GFP
C47A-GFP
C51A-GFP
C67A-GFP
C75A-GFP
C87A-GFP
10 days
15 days

B

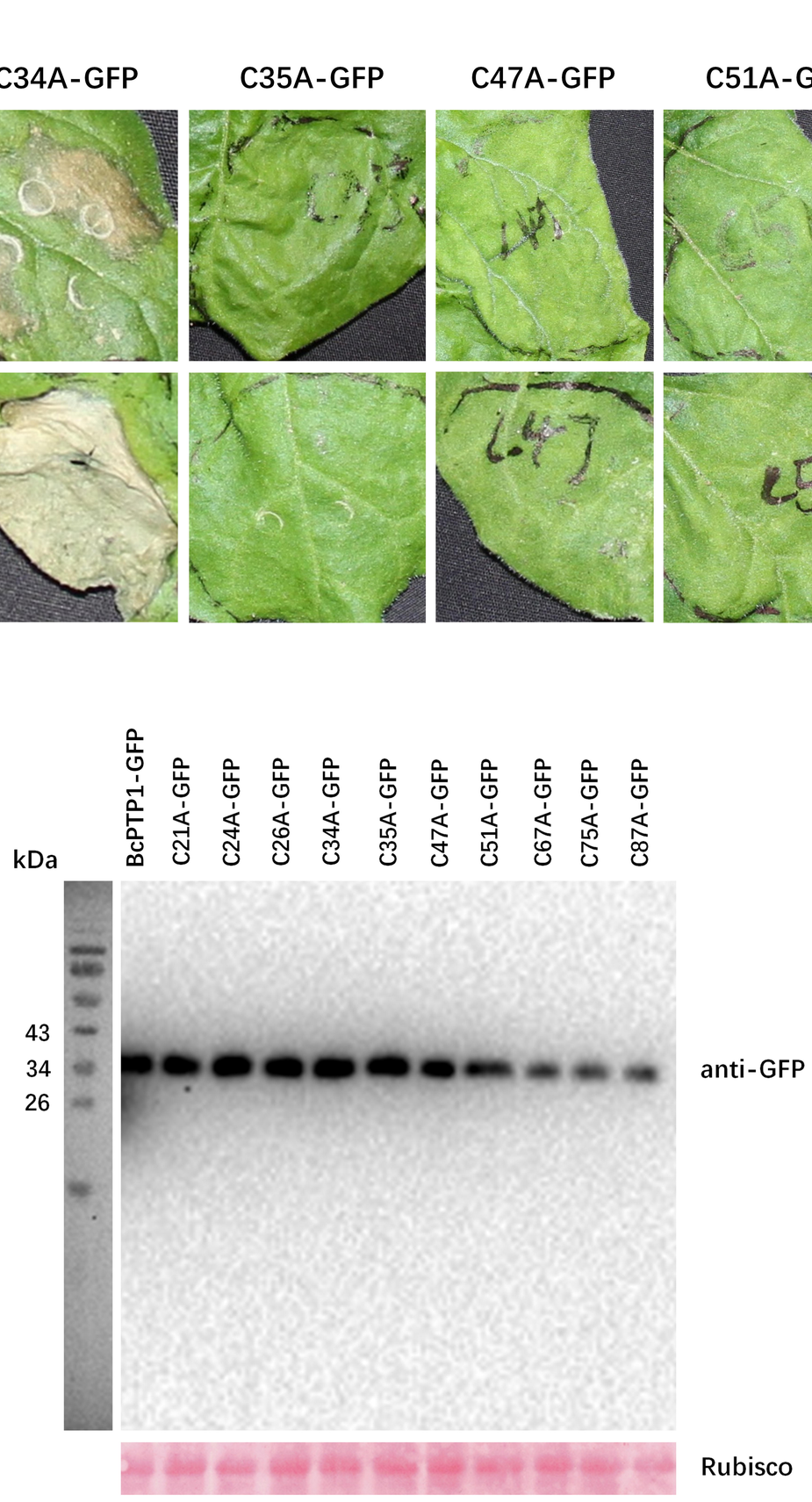
kDa
BcPTP1-GFP
C21A-GFP
C24A-GFP
C26A-GFP
C34A-GFP
C35A-GFP
C47A-GFP
C51A-GFP
C67A-GFP
C75A-GFP
C87A-GFP
43
34
26
anti-GFP
Rubisco

100°C treated

25°C treated

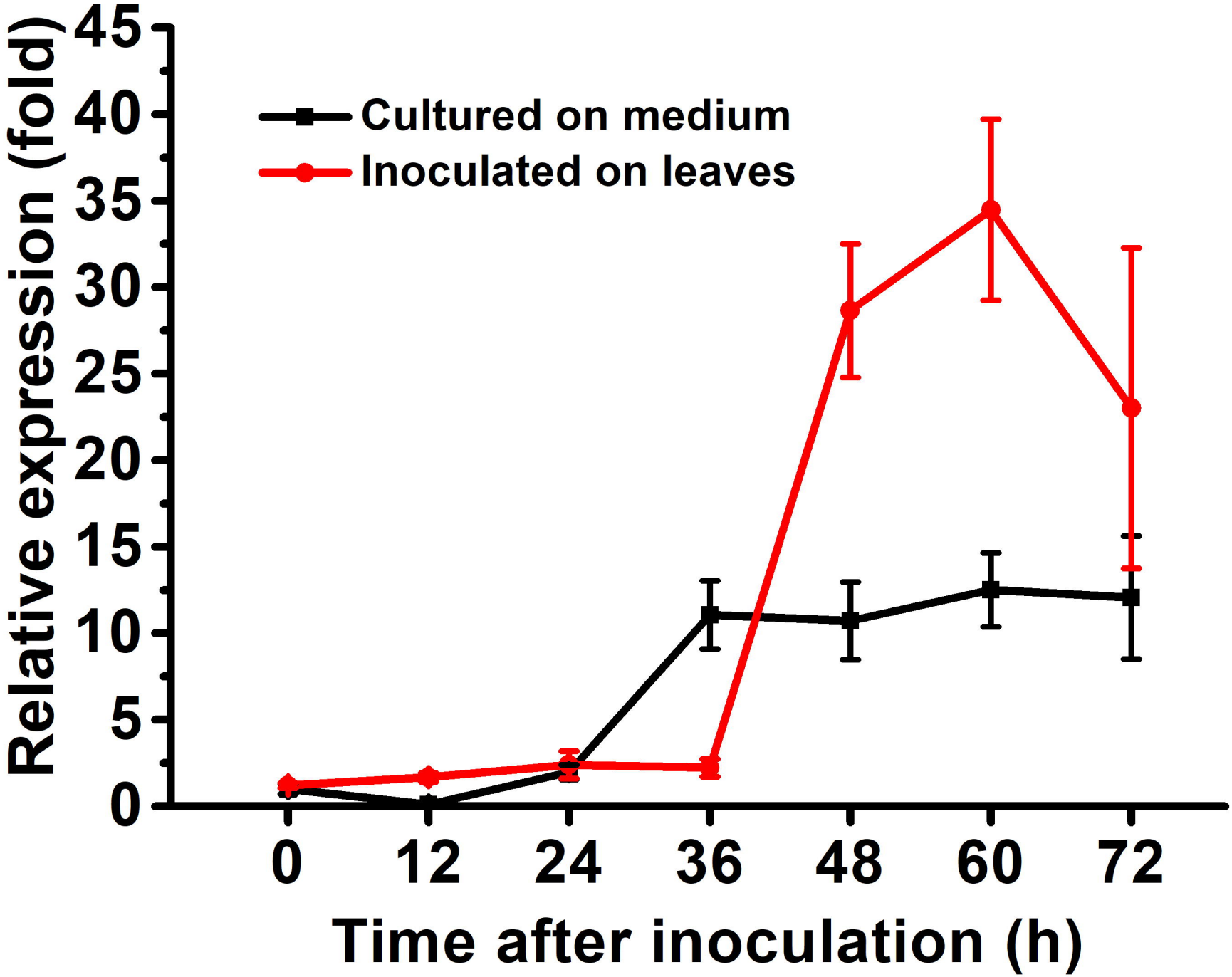
Relative expression (fold)
45
40
35
30
25
20
15
10
5
0
Cultured on medium
Inoculated on leaves
0
12
24
36
48
60
72
Time after inoculation (h)

A

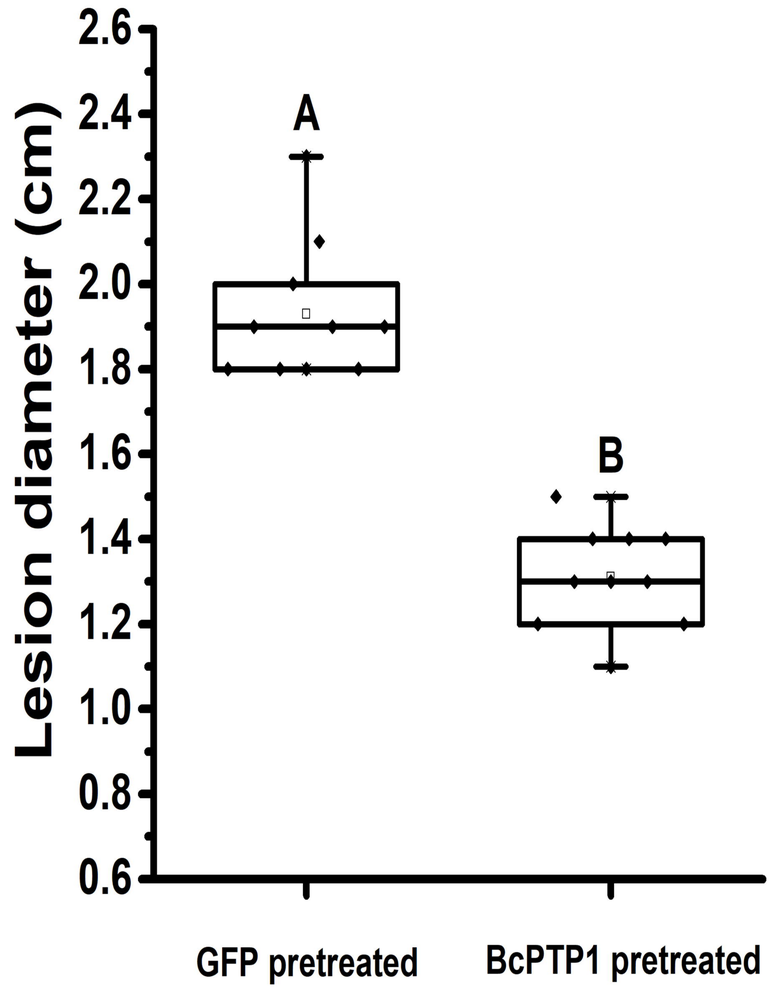

B

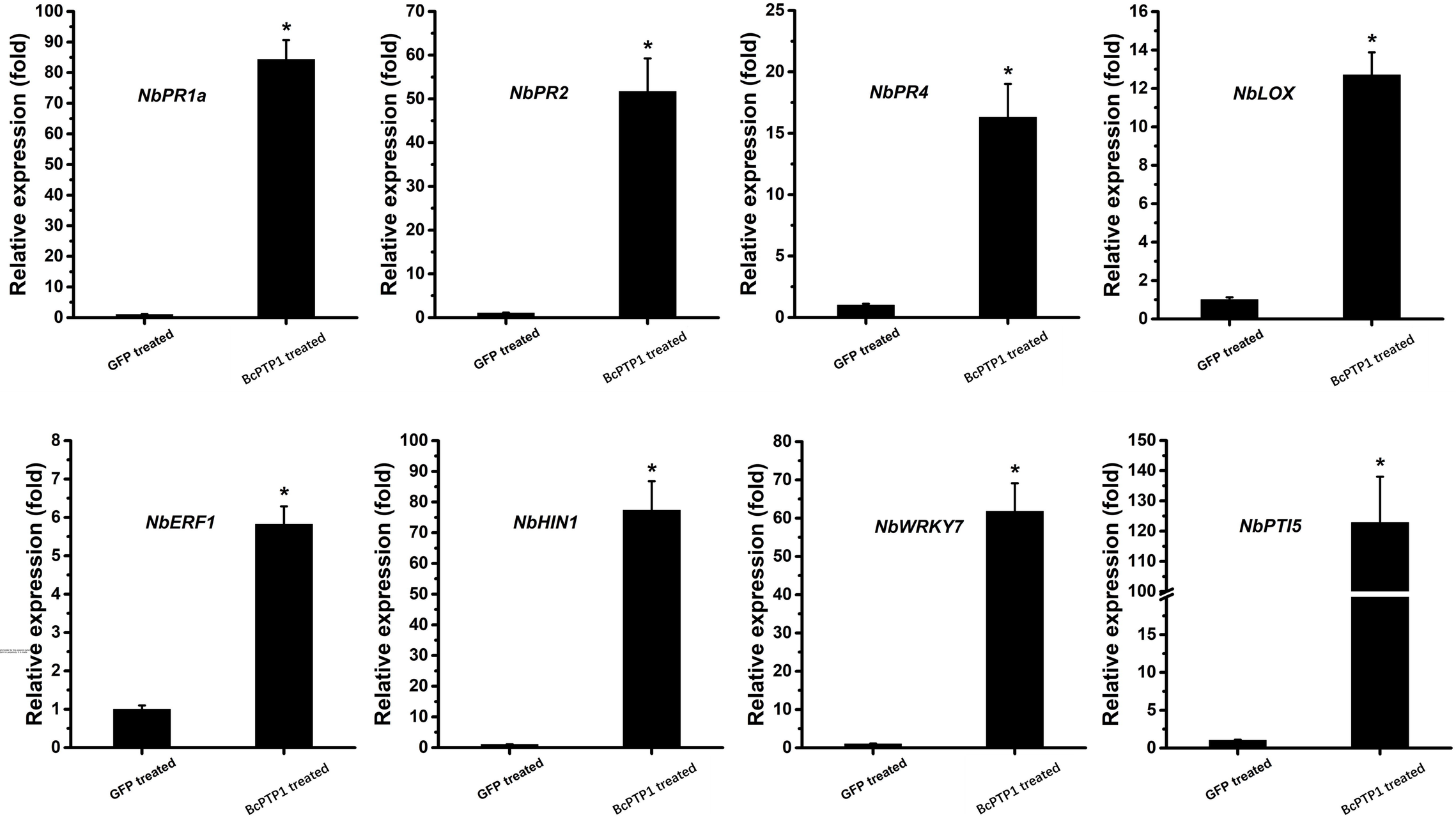

A

B

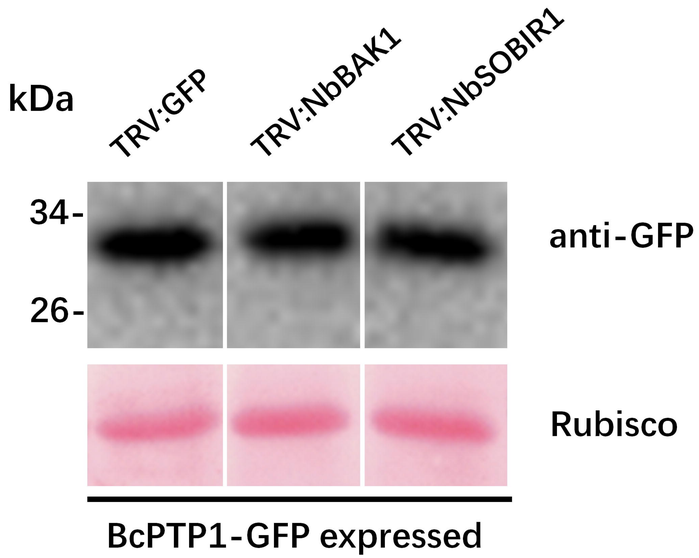

C

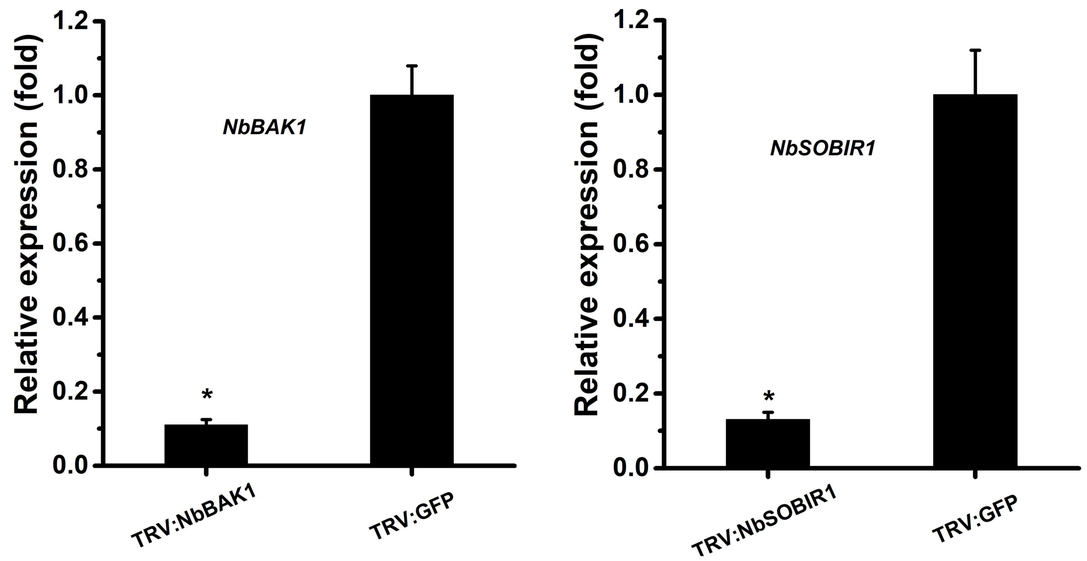

Apoplast

Plant cell

Botrytis cinerea

BcPTP1

Secretion

SOBIR1

Unknown Receptor

BAK1

Internalization

RLP or RLK

Defense

RLP or RLK

Phytotoxicity